



# Macroscopic quantum simulation of high-order harmonic generation in a gas jet, using upgraded 1D atomic model potentials

Krisztina Sallai, Szilárd Majorosi, Szabolcs Hack, Attila Czirják

ELI ALPS, Theory and Simulations Group & University of Szeged, Dept. of Theoretical Physics,  
Szeged, Hungary

GPU Day 2026,  
HUN-REN Centre, Budapest, May 29, 2026.





**Krisztina Sallai, PhD student**



**Dr. Szabolcs Hack, PhD**



**Dr. Szilárd Majorosi, PhD**

- ELI ALPS, HHG, attosecond pulses
- MMA-HHG code structure
- 3D vs 1D simulations in strong-field physics
- Upgraded 1D soft-core Coulomb potential (GSC)
- Preliminary numerical results from Komondor
- Conclusions and outlook



# ELI: Extreme Light Infrastructure

International user facility for researchers of various disciplines.

ELI is a **distributed research infrastructure**

- Hungary (ELI-ALPS)
- Czech Republic (ELI Beamlines)
- Romania (ELI-NP)

ELI ALPS is concluding the Implementation Phase (co-financed by European Regional Development Fund), which is managed by ELI-Hu Nonprofit Ltd.

## ELI ERIC

To **provide access** for European and international researchers to the ELI Facilities in the Czech Republic and Hungary. Integrating the ELI facilities, and move to the Operational Phase

## ALPS: Attosecond Light Pulse Source, Szeged

To generate femtosecond and attosecond pulses, for temporal investigations of electron dynamics in atoms, molecules, plasmas and solids.



# ELI ALPS Portfolio of research opportunities

## Capacity, Capability and Uniqueness

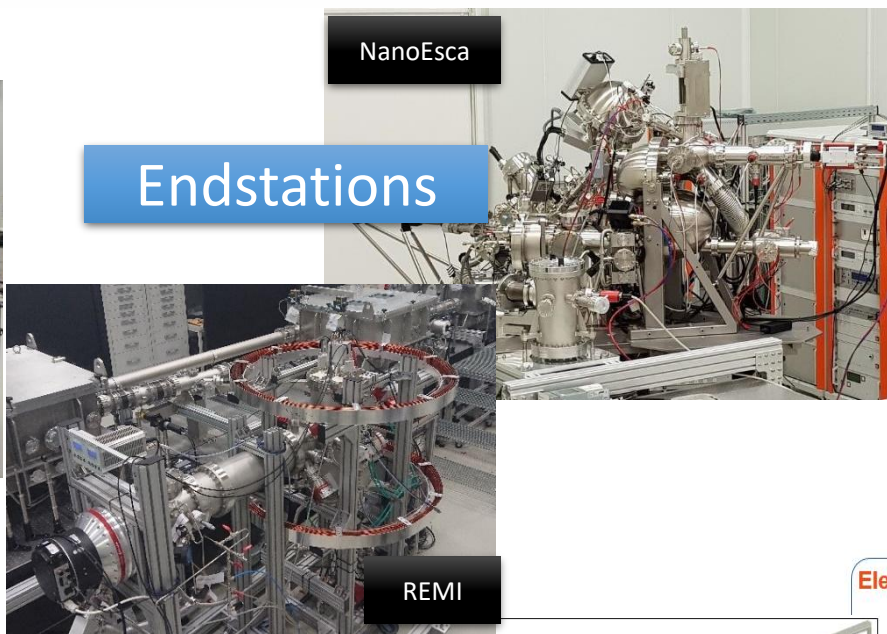


### Lasers



### NanoEsca

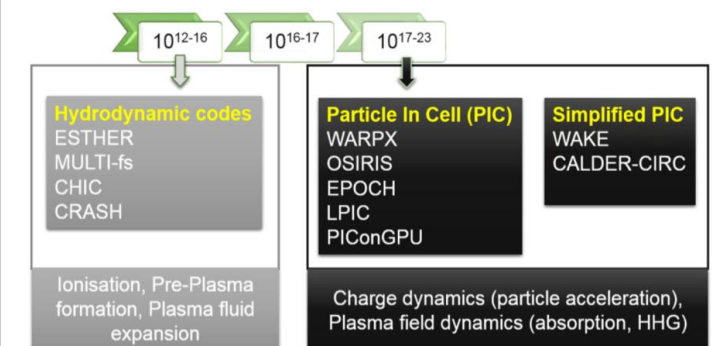
### Endstations



### REMI

### Simulation tools

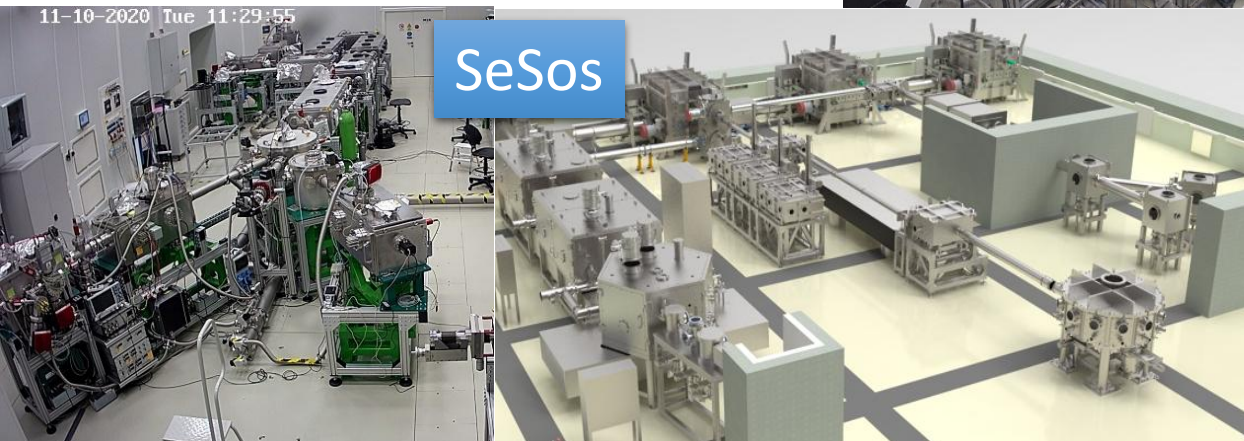
Simulation tools in intense laser matter interaction



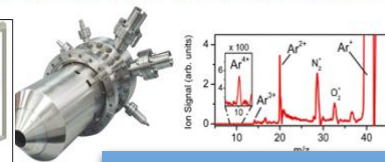
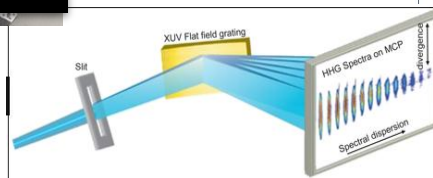
Featured in p19-20 [https://hpc.kifu.hu/sites/default/files/2021-06/HPC\\_Echo\\_2021.pdf](https://hpc.kifu.hu/sites/default/files/2021-06/HPC_Echo_2021.pdf)

11-10-2020 Tue 11:29:55

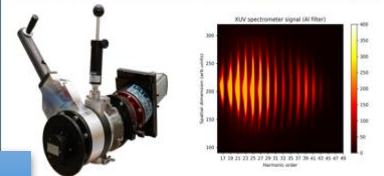
### SeSos



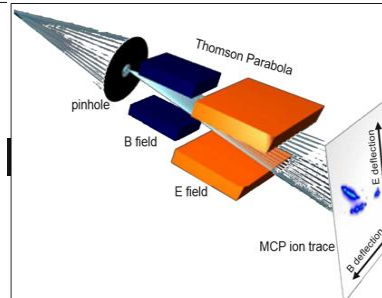
### Electron/Ion TOF (5x + high resolution)



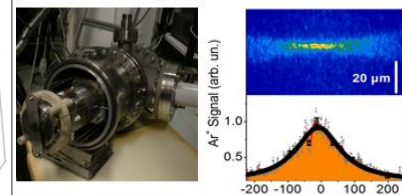
### XUV/VUV Photon spectrometer (5x)



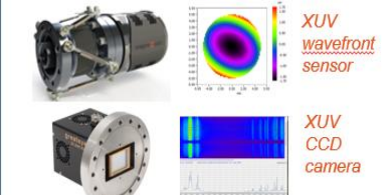
### Metrology



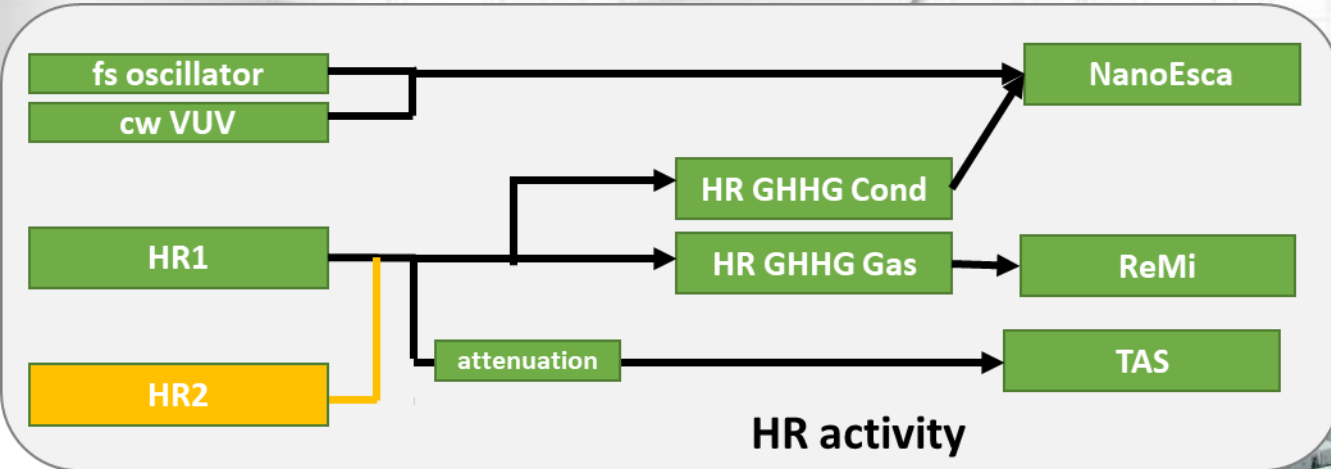
### Ion Microscope (2x)



### Beam diagnostics



# HR GHHG beamlines: attosecond physics



**HR2**  
100 kHz, 7 fs, 5 mJ

activefiber systems

- 6 mJ, 76 fs or 9 fs, 3.5 mJ
- problems with beam profile
- CEP stability not addressed
- Development ongoing in Szeged

**HR1**  
100 kHz, 7 fs, 1 mJ

activefiber systems

- in user service
- CEP locking @ 600 mrad

**HR Condensed + NanoEsca**

CNRIFN Istituto di Fotonica e Nanotecnologie scientaomicron

- beamline commissioned
- monochromatized XUV pulses
- XUV-IR experiments with NanoEsca

**HR Gas + ReMi**

CNRIFN Istituto di Fotonica e Nanotecnologie RoentDek UUV-Detectors Sparsomic Gas Jets Multifragment Imaging Systems

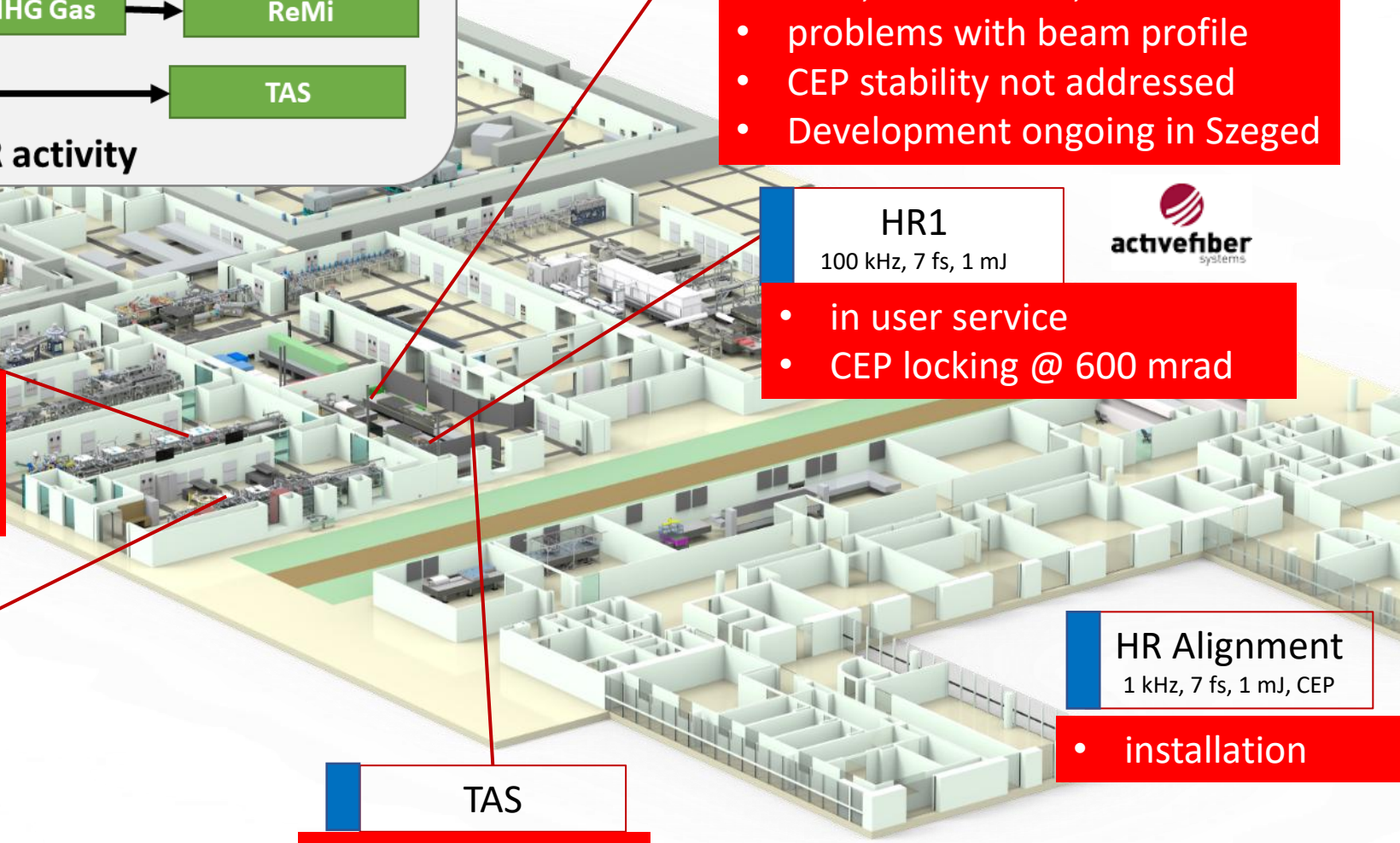
- ReMi installed
- XUV-IR experiments

**TAS**

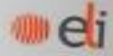
- commissioned

**HR Alignment**  
1 kHz, 7 fs, 1 mJ, CEP

- installation

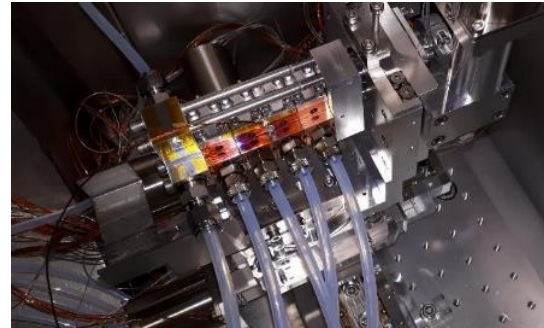
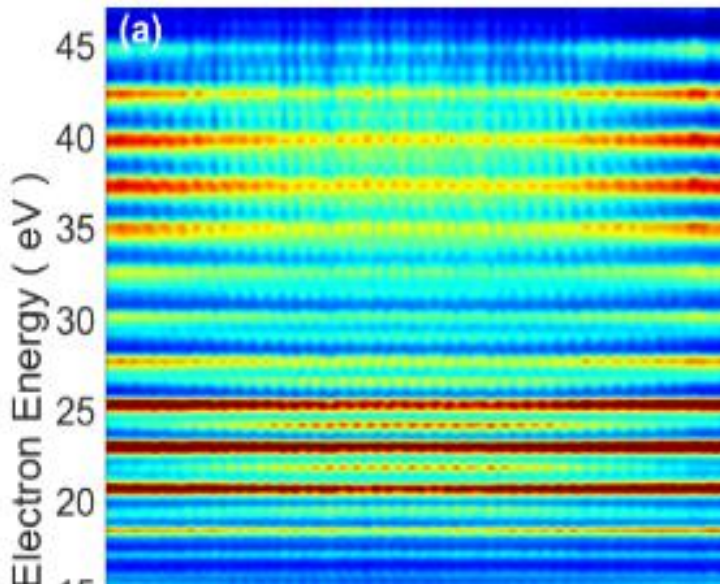


# HR GHHG beamlines: attosecond physics



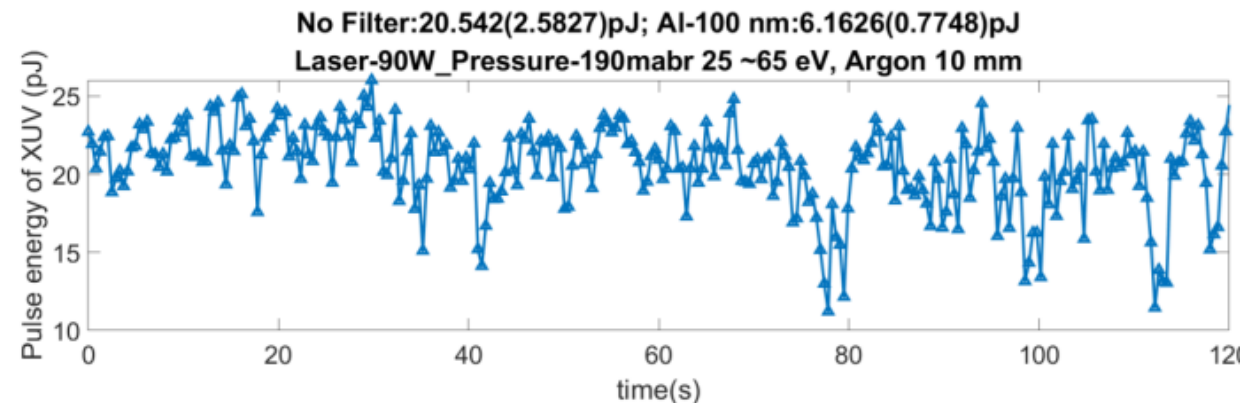
- **XUV-IR pump-probe** studies on **gaseous and condensed targets** at **100 kHz**
- diagnostics for the temporal, spectral and spatial characterization of the XUV pulses
- **flexible reconfiguration** according to user needs
- specially designed, cooled static HHG cell

Designed by:  CNR IFN  
Istituto di Fotonica e Nanotecnologie



**~166 as,**  
**~250 pJ generated,**  
**~50 pJ on target @ 100 kHz**

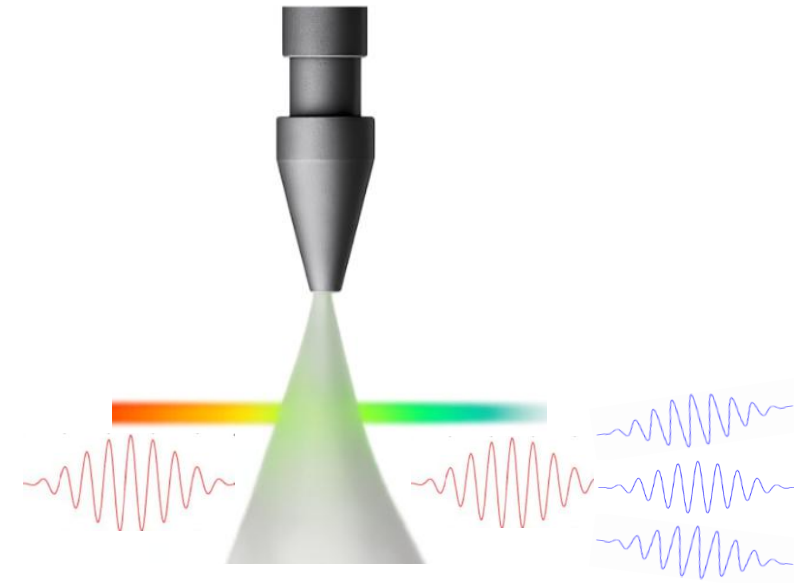
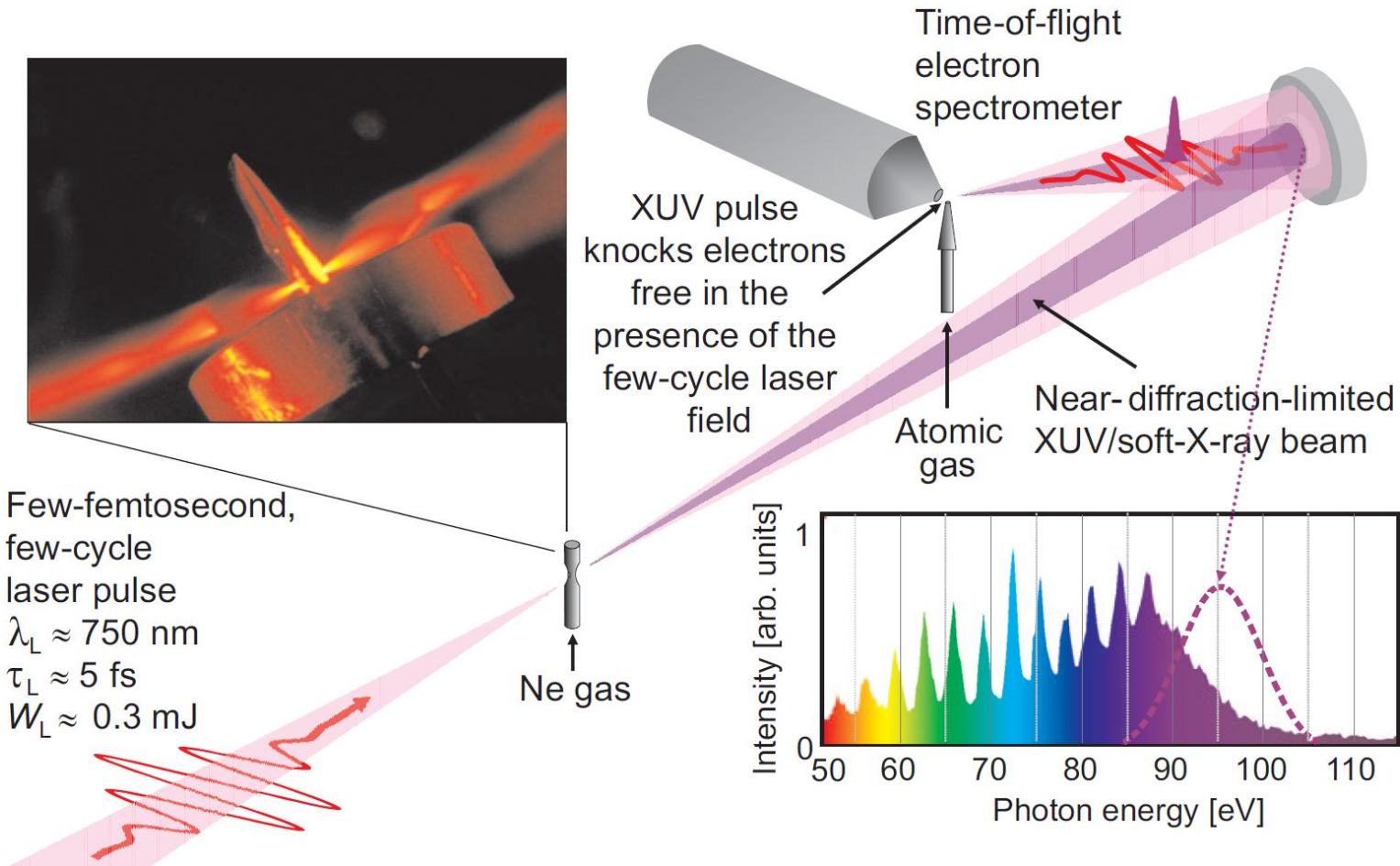
## Highest flux attosecond pump-probe beamline @ 100 kHz



Peng Ye *et al.*, *J. Phys. B: At. Mol. Opt. Phys.* **53** 154004 (2020)

Peng Ye *et al.*, *Ultrafast Science* 2022, 9823783 (2022)

# Our simulation goal: HHG in a gas jet



# Structure of the MMA-HHG code

Jan Vábek, Tadeás Nemeč, Stefan Skupin, Fabrice Catoire

CUPRAD

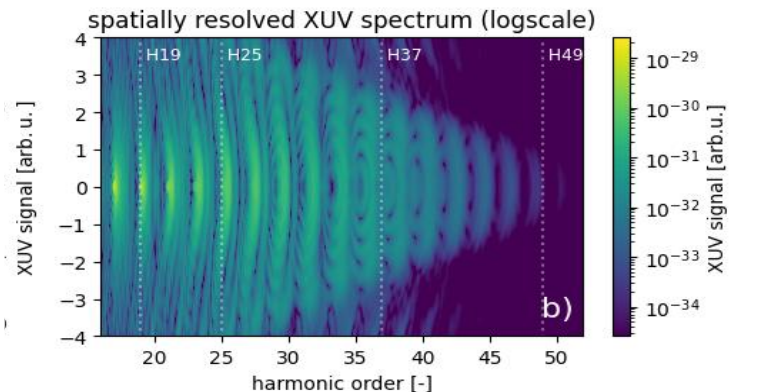
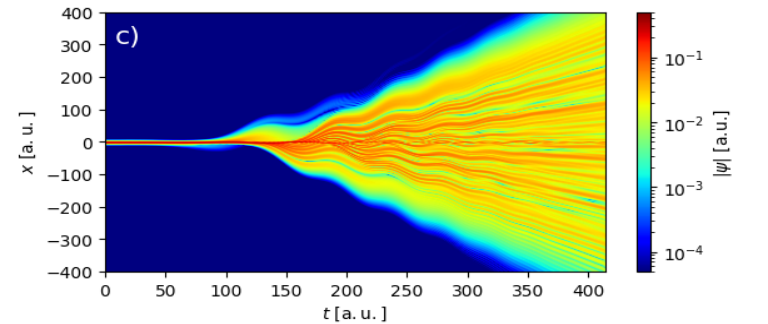
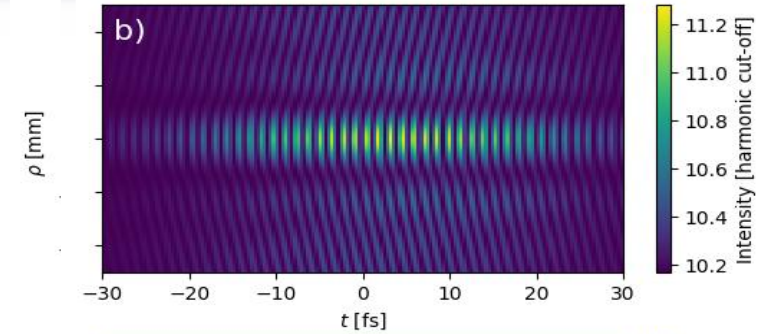
- Parallel Radially Symmetric Unidirectional Solver
- Non-linear laser propagation

TDSE

- 1D-TSDE Implementation
- Microscopic response, using SC atomic model pot.

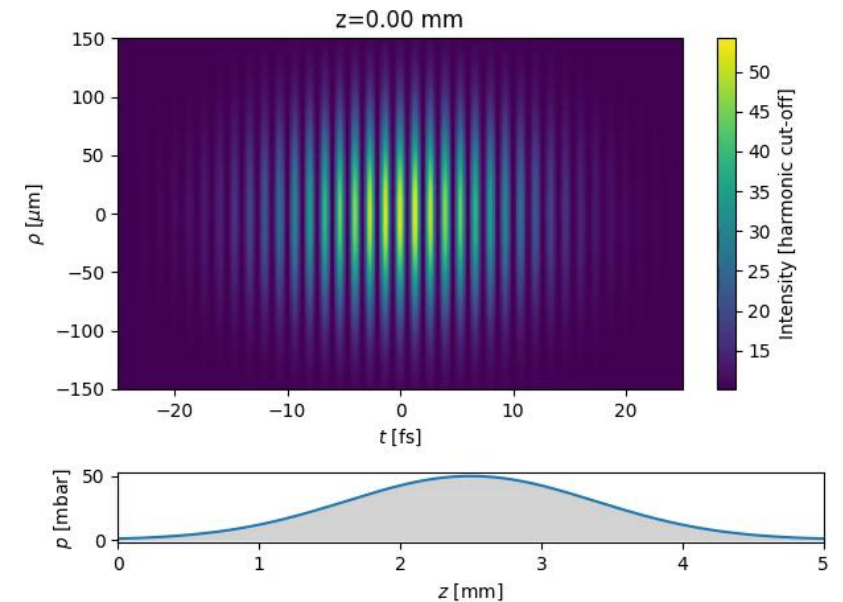
HANKEL

- Linear XUV Propagator
- XUV propagation



## CUPRAD – Non-linear Laser Pulse Propagation

- Simulates macroscopic laser propagation
- Linear polarisation
- Cylindrical symmetry
- SVEA approximation
- Split-step scheme
- Includes Kerr response



An illustration of the non-linear propagation of a laser pulse in an argon jet (Gaussian profile bottom panel)

## TDSE – Microscopic response

- Solves time-dependent Schrödinger equation
- 1D single-active-electron model (SC)
- Driven by local electric field  $E(t)$
- Outputs dipole acceleration
- Parallel over spatial grid points
- Crank-Nicolson scheme

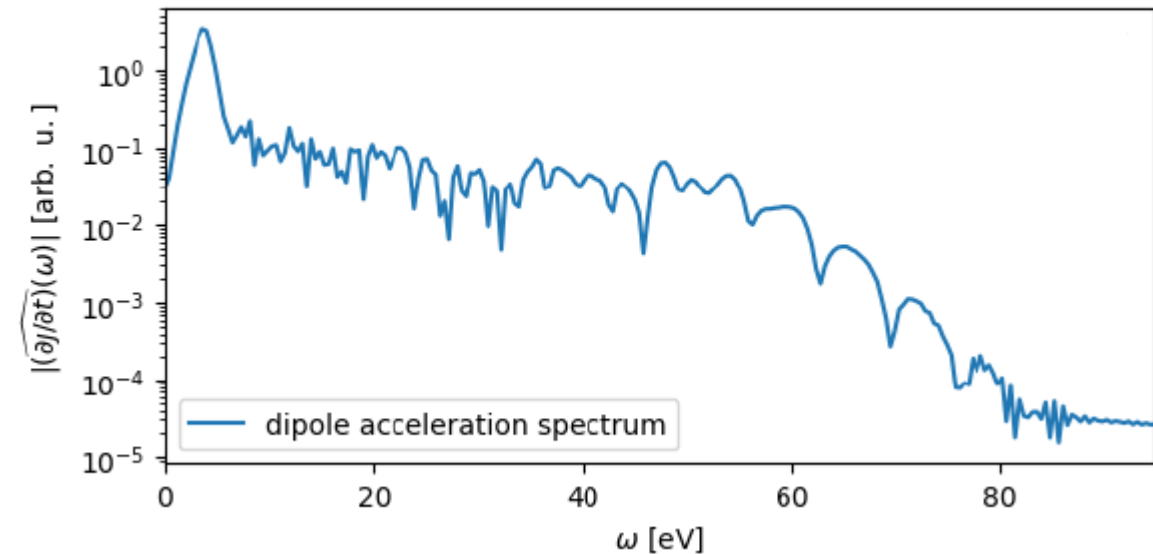
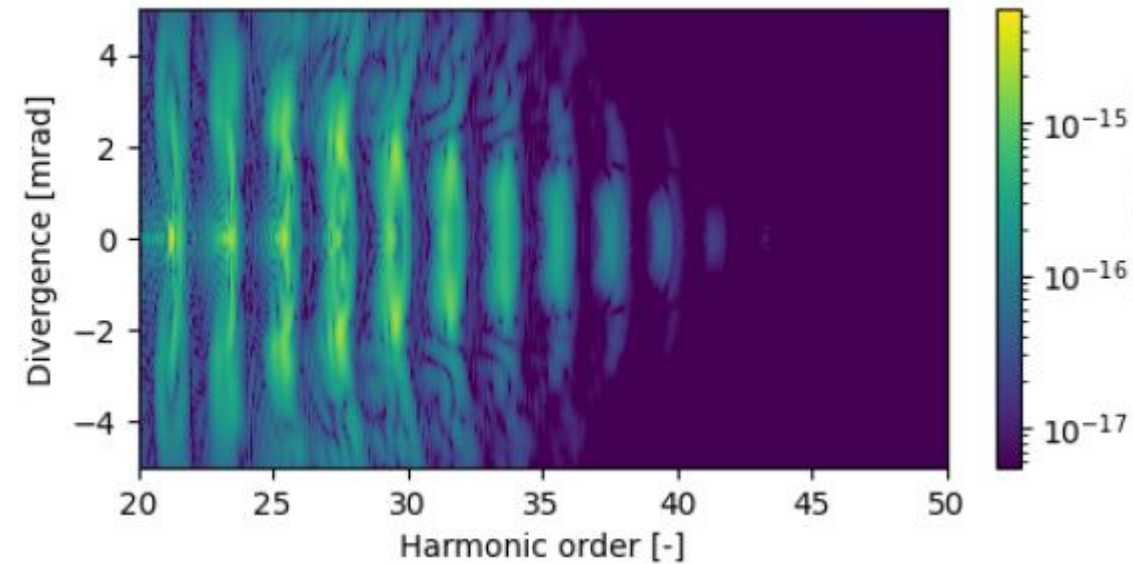


Illustration of a 1D dipole acceleration spectrum

## Hankel – XUV far-field propagation

- Linear propagation of XUV radiation
- Diffraction integral
- Hankel transform (cylindrical symmetry)
- Includes phase matching and absorption
- Outputs far-field spectrum and spatial profile



An illustration of spatially resolved far-field harmonic spectra

# Theory of strong-field ionization



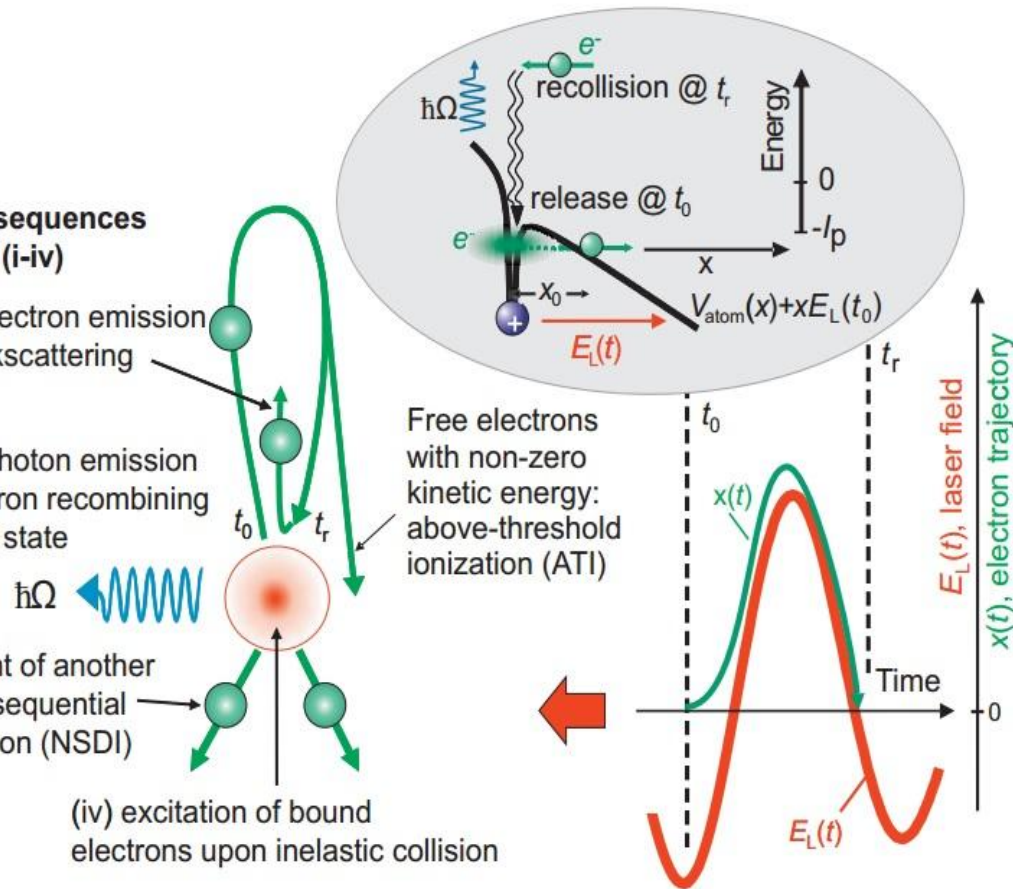
## Possible consequences of recollision (i-iv)

(i) energetic electron emission by elastic backscattering of the electron

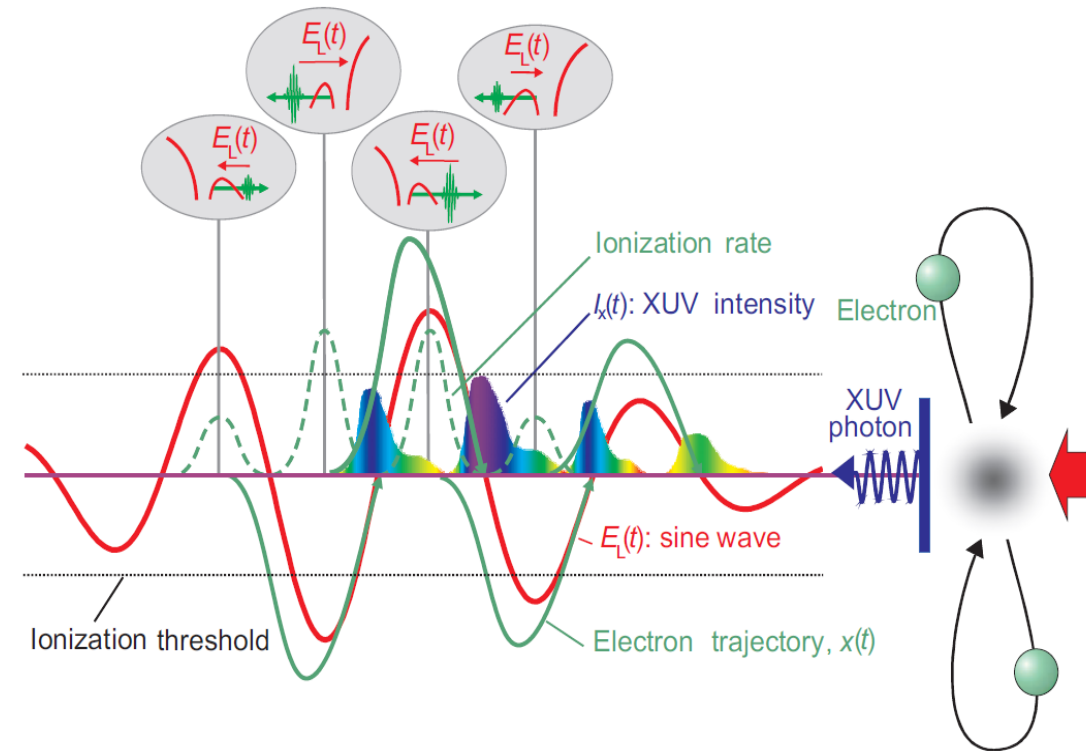
(ii) energetic photon emission upon the electron recombining into its ground state

(iii) detachment of another electron: non-sequential double ionization (NSDI)

(iv) excitation of bound electrons upon inelastic collision



Free electrons with non-zero kinetic energy: above-threshold ionization (ATI)



# Theoretical framework

## SAE atom, dipole approximation

Few-cycle laser pulse:

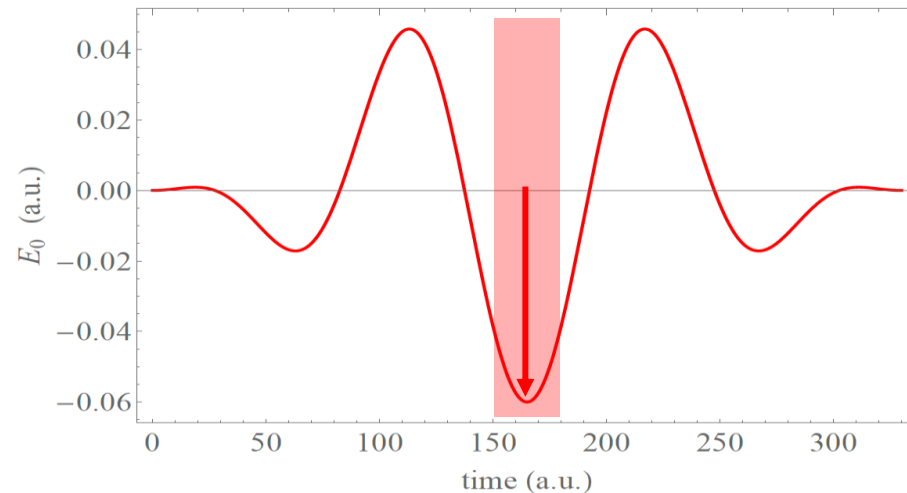
$$\mathcal{E}_z(t) = F \cdot \sin^2 \left( \frac{\pi t}{NT} \right) \cos \left( \frac{2\pi t}{T} + \phi \right)$$

Keldysh parameter:  $\gamma \sim 1$

Usual parameters:

$$F = 0.06, N = 3, T = 110, \phi = 0$$

$$I \sim 100 \text{ TW/cm}^2, \lambda \approx 800 \text{ nm}$$



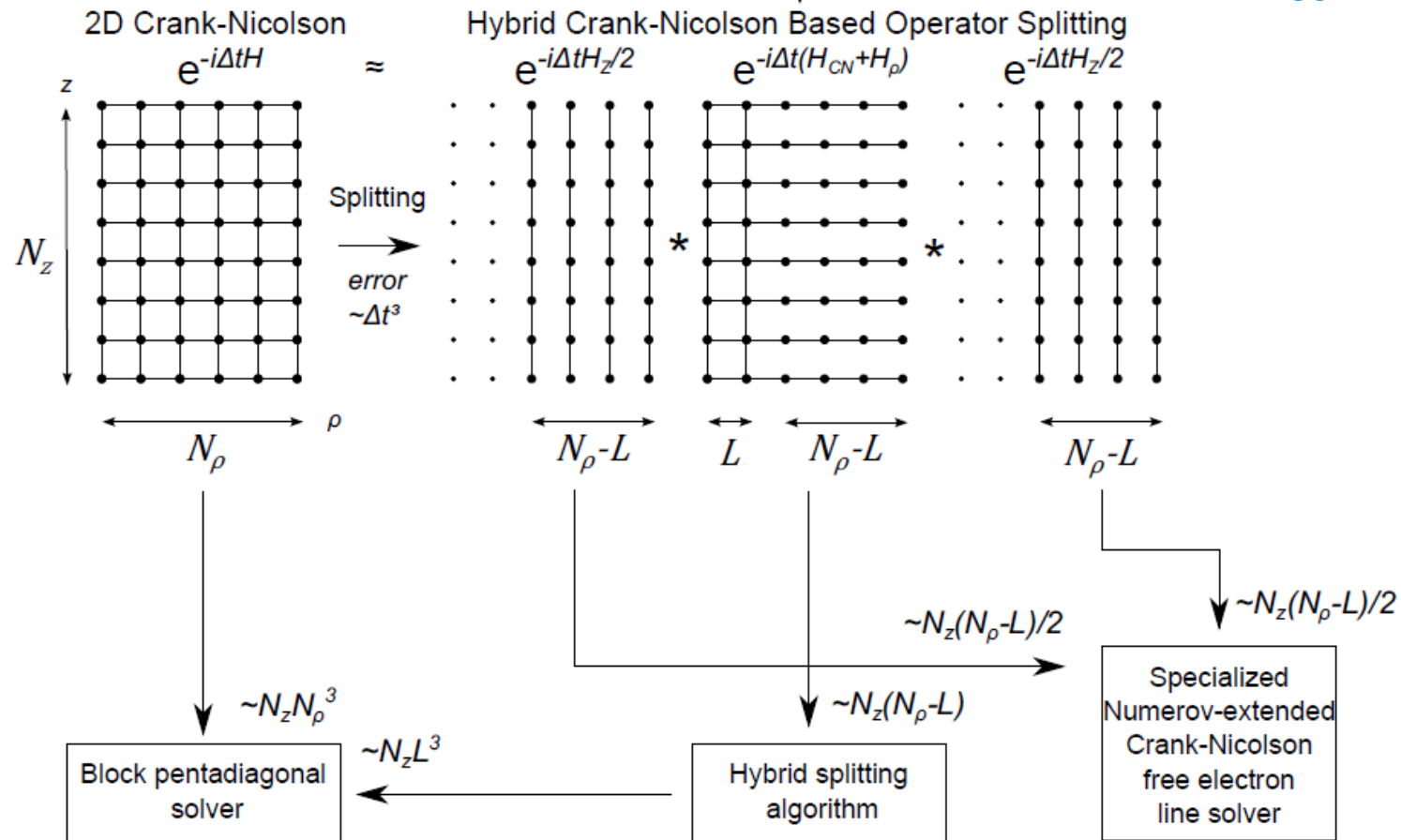
3D Schrödinger equation in cylindrical coordinates and in length gauge:

$$i \frac{\partial}{\partial t} \Psi(z, \rho, t) = \left[ -\frac{1}{2} \left( \frac{\partial^2}{\partial z^2} + \frac{\partial^2}{\partial \rho^2} + \frac{1}{\rho} \frac{\partial}{\partial \rho} \right) - \frac{1}{\sqrt{z^2 + \rho^2}} + \mathcal{E}_z(t) \cdot z \right] \Psi(z, \rho, t)$$

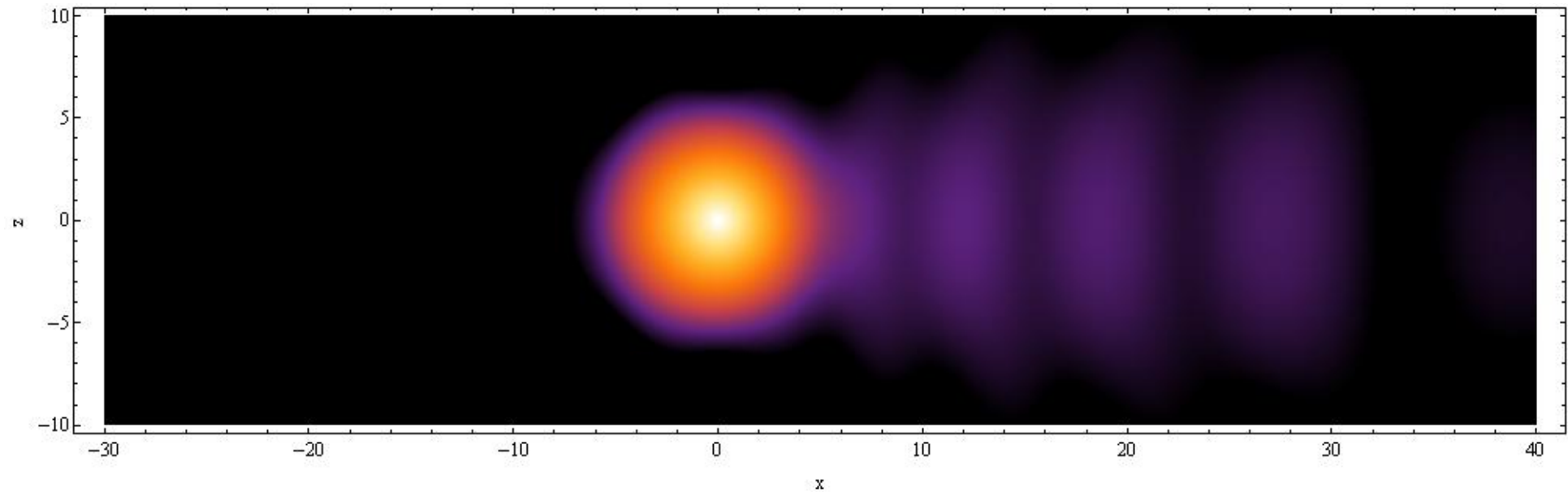
# Accurate and effective numerical algorithm for 3D H-atom driven by a strong lin. pol. laser pulse

High order iterative splitting formulas

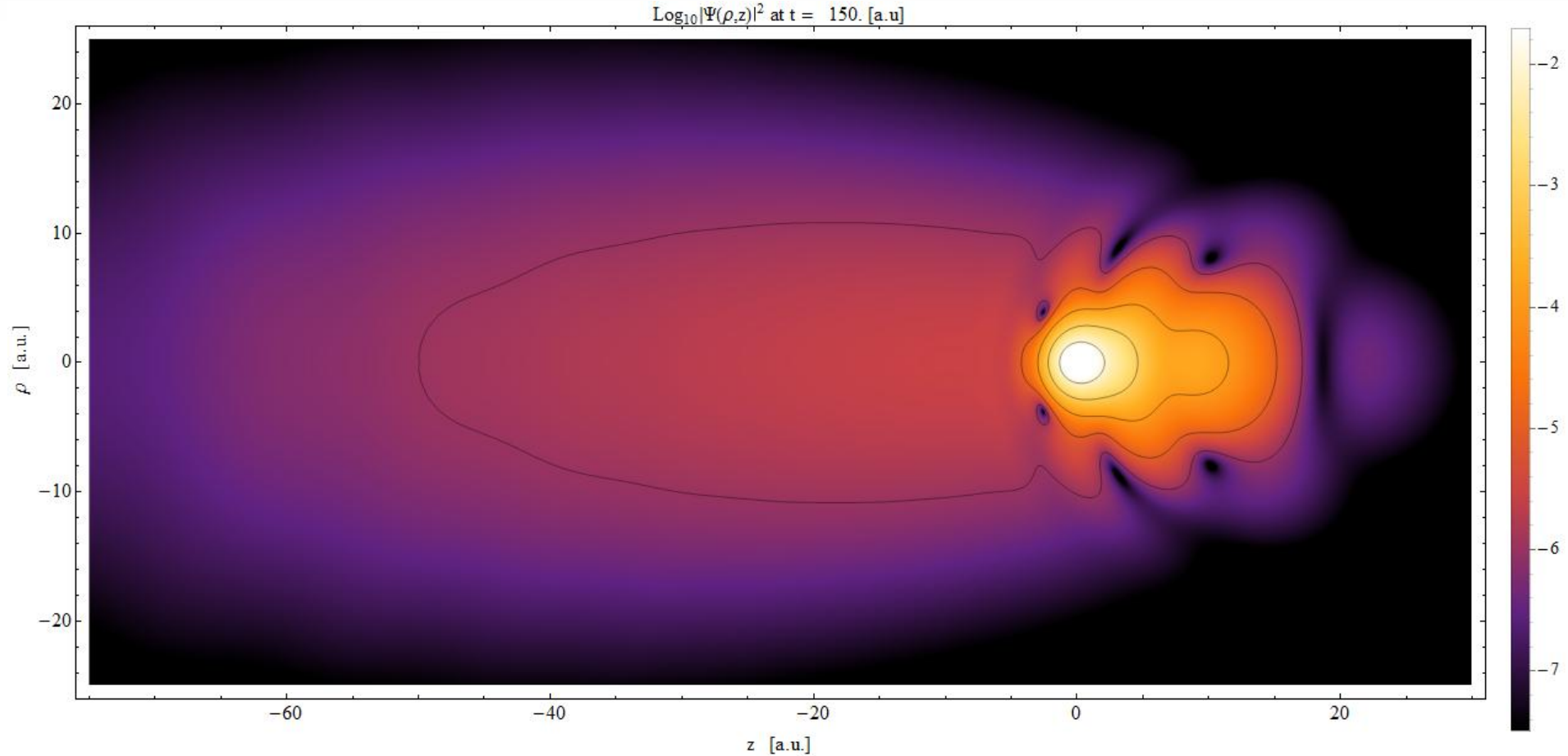
Sz. Majorosi and A. Czirják, *Comp. Phys. Comm.* **208**, 9-28, (2016)



# Typical numerical results in 3D: Strong-field ionization of atomic H, lin. pol. NIR fs pulse



# Typical numerical results in 3D: Strong-field ionization of atomic H, lin. pol. NIR fs pulse



# 3D vs 1D simulations in strong-field physics



3D, cylindrical coordinates:

$$i \frac{\partial}{\partial t} \Psi^{3D}(z, \rho, t) = [H_0^{3D} + V_{\text{ext}}(z, t)] \Psi^{3D}(z, \rho, t)$$

$$H_0^{3D} = T_z + T_\rho - \frac{Z}{\sqrt{\rho^2 + z^2}} \quad V_{\text{ext}}(z, t) = z \cdot \mathcal{E}_z(t)$$

1D, along z-axis, parallel with laser polarization:

$$i \frac{\partial}{\partial t} \Psi^{1D}(z, t) = [H_0^{1D} + V_{\text{ext}}(z, t)] \Psi^{1D}(z, t)$$

$$H_0^{1D} = T_z + V_0^{1D}(z) \quad V_{\text{ext}}(z, t) = z \cdot \mathcal{E}_z(t)$$

**Good 1D model: good match of 1D and 3D physical quantities, using the same laser field**

# Construction of the density-based 1D model potential

3D ground state:  
(Z: effective ion-core charge)  $H_0^{3D} \psi_{100}(z, \rho) = E_0 \psi_{100}(z, \rho) \quad E_0 = -\frac{\mu Z^2}{2}, \quad \psi_{100}(z, \rho) = \mathcal{N} e^{-\mu Z \sqrt{\rho^2 + z^2}}$

Reduced ground state density:  $\rho_z^{100}(z) = 2\pi \int_0^\infty |\psi_{100}(z, \rho)|^2 \rho d\rho = \frac{\mu Z}{2} (2Z\mu|z| + 1) e^{-2Z\mu|z|}$

**Idea: Let 1D ground state density be identical to reduced ground state density!**

1D ground state wave function:

$$\psi_0(z) = \sqrt{\frac{\mu Z}{2}} \sqrt{2\mu Z|z| + 1} e^{-\mu Z|z|}$$

Substitute the ground state into 1D Schrödinger eq. and solve for the potential:

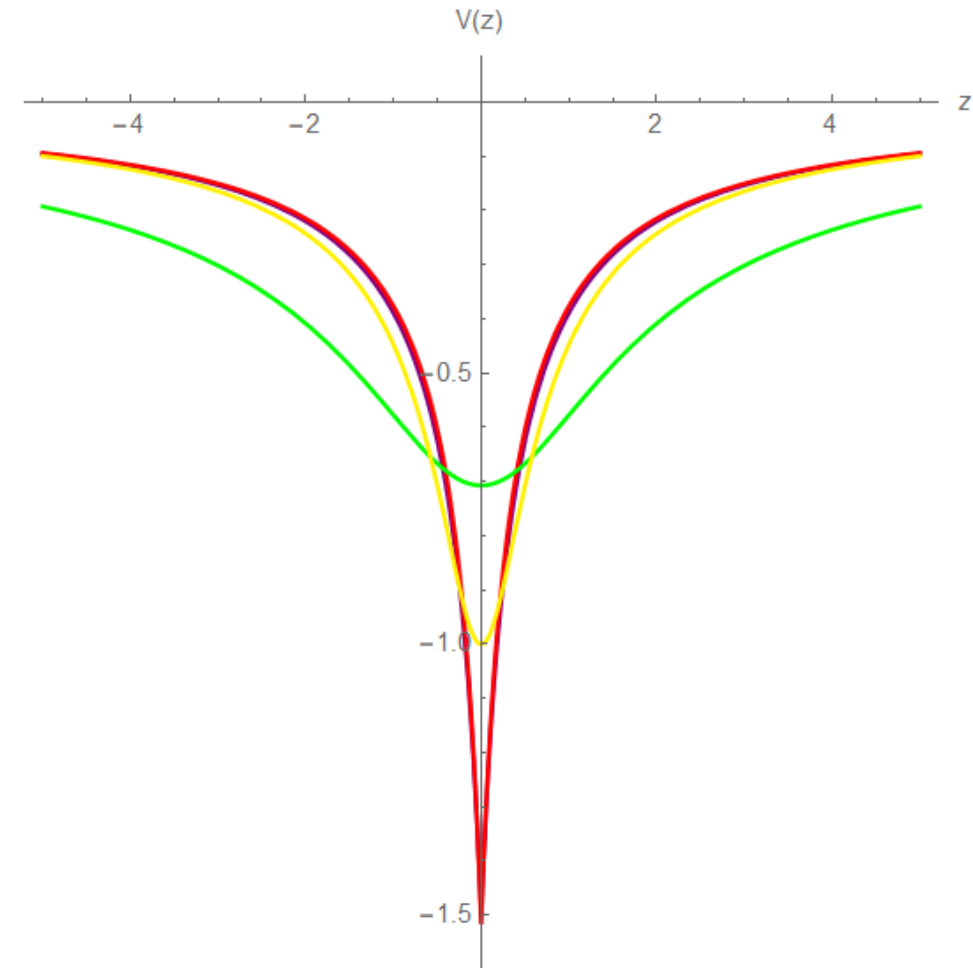
$$V_{0,M}^{1D}(z) = E_{0,M} + \frac{1}{\psi_0(z)} \frac{1}{2\mu} \frac{\partial^2}{\partial z^2} \psi_0(z) \quad \lim_{|z| \rightarrow \infty} V_{0,M}^{1D}(z) = 0$$

The density-based 1D model potential (red curve):

$$V_{0,M}^{1D}(z) = -\frac{1}{2\mu} \frac{1}{2^2 \left(|z| + \frac{1}{2\mu Z}\right)^2} - \frac{\frac{1}{2}Z}{|z| + \frac{1}{2\mu Z}}$$

Improved soft-core Coulomb potential (MSC potential, yellow curve):

$$V_{0,M,Sc}^{1D}(z) = -\frac{\frac{1}{2}Z}{\sqrt{z^2 + \frac{1}{4Z^2}}}$$



# Improved 1D model potentials for H and simulation results

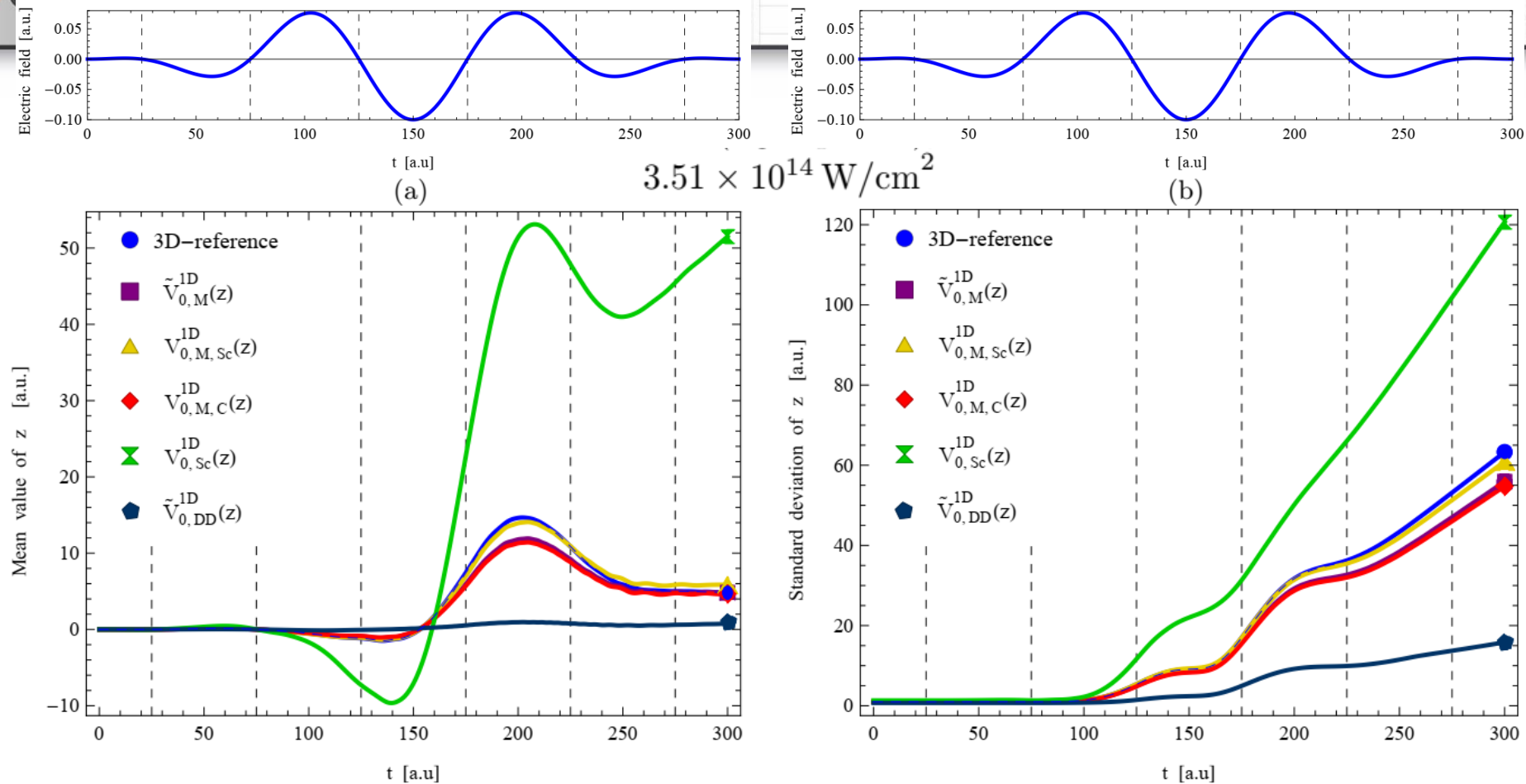


Figure 2. Time-dependence of the mean values  $\langle z \rangle(t)$  (a) and the standard deviations  $\sigma_z(t)$  (b) using different 1D model potentials, under the influence of the same external field with  $F = 0.1$ ,  $N_{\text{Cycle}} = 3$  and  $T = 100$ . Results of the corresponding 3D simulation are plotted in blue.

HHG spectra of H: scaling of the power spectrum needed  $3.51 \times 10^{14} \text{ W/cm}^2$

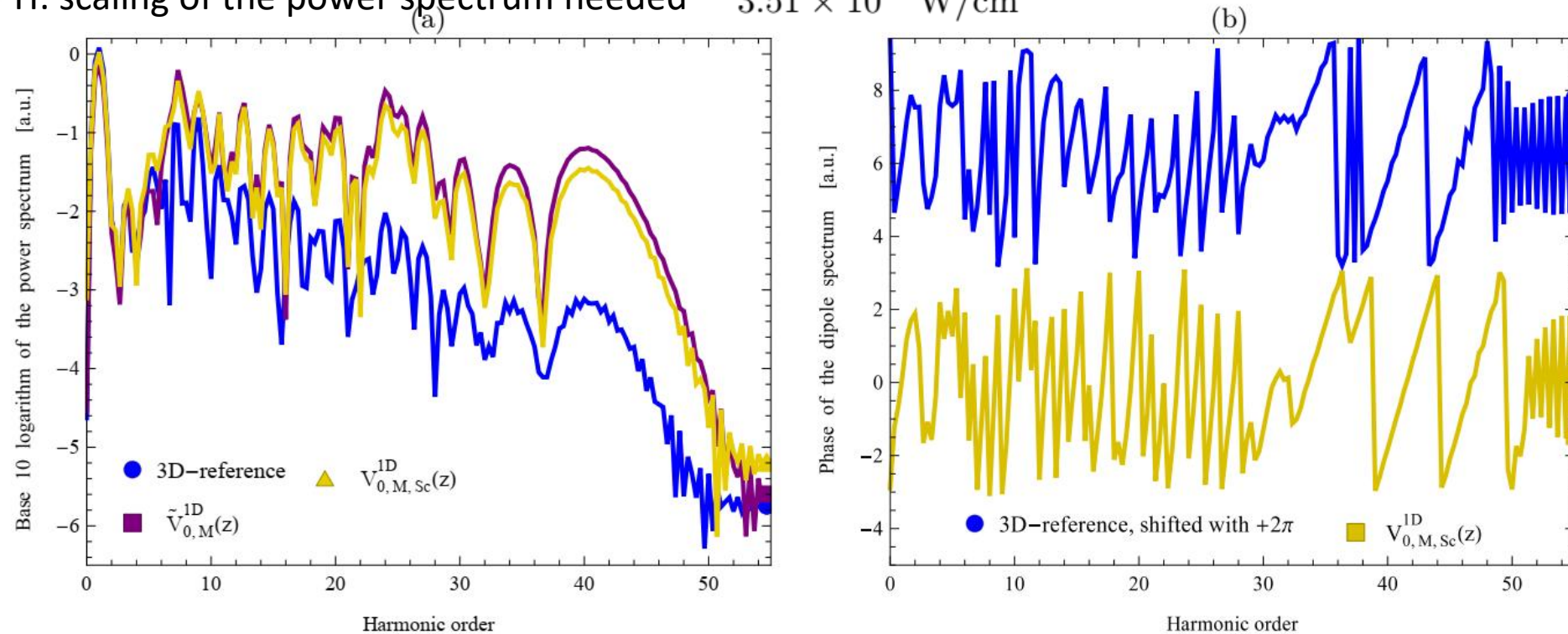
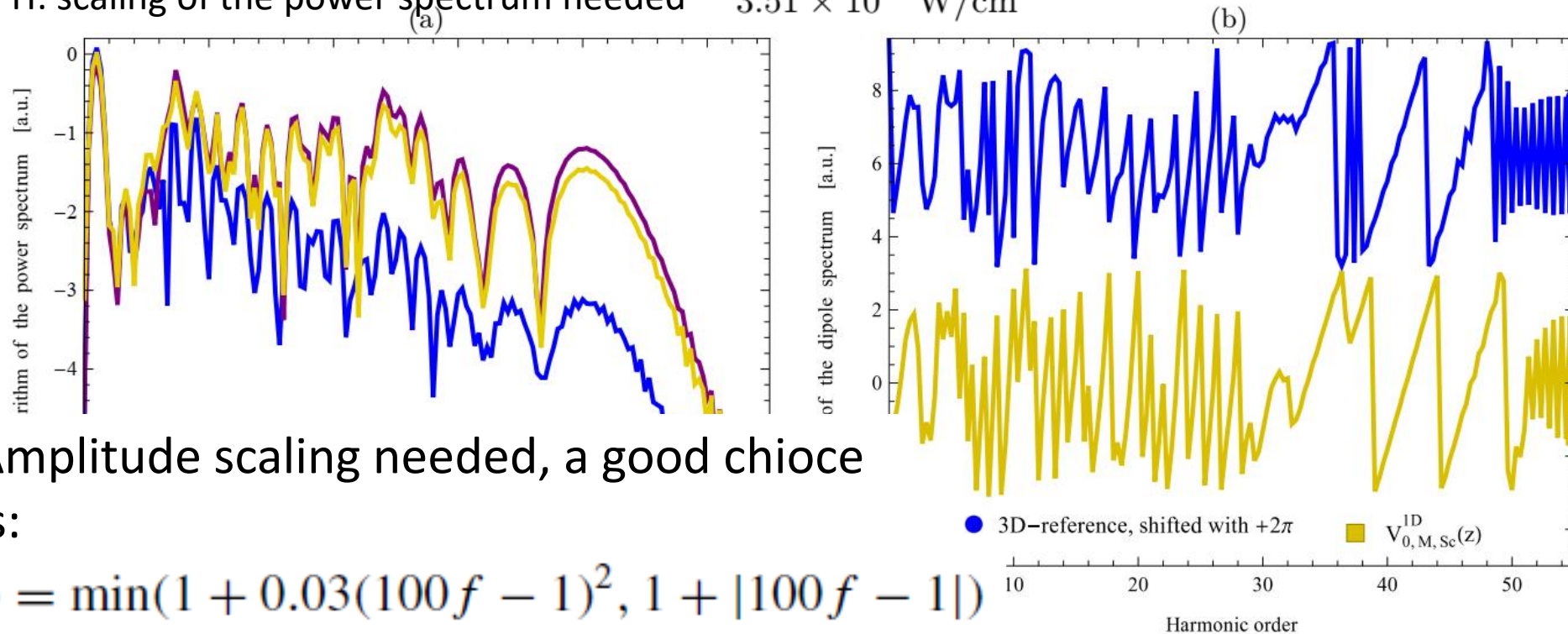


Figure 6. Panel (a): Logarithmic plot of the power spectra vs. the harmonic order, i.e.  $p(nf_1)$  (where  $f_1 = 1/T = 0.01$  a.u. is the fundamental frequency). Panel (b): Phase of the dipole acceleration spectra vs. the harmonic order (up shifted by  $2\pi$  for the 3D case). We plot the results for the density-based 1D model potential (purple) and for the improved soft-core Coulomb potential (gold) in comparison with the 3D reference (blue). The parameters  $F = 0.1$ ,  $N_{\text{Cycle}} = 3$ ,  $T = 100$  and  $Z = 1$  are the same as for Figs. 2 and 3.

HHG spectra of H: scaling of the power spectrum needed  $3.51 \times 10^{14} \text{ W/cm}^2$



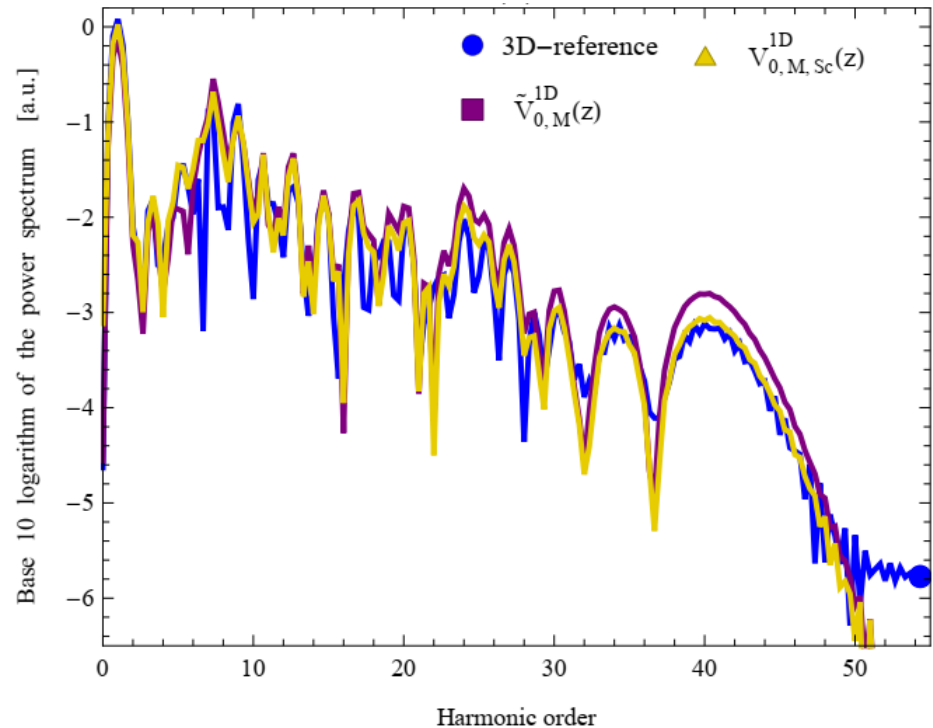
Amplitude scaling needed, a good choice is:

$$s(f) = \min(1 + 0.03(100f - 1)^2, 1 + |100f - 1|)$$

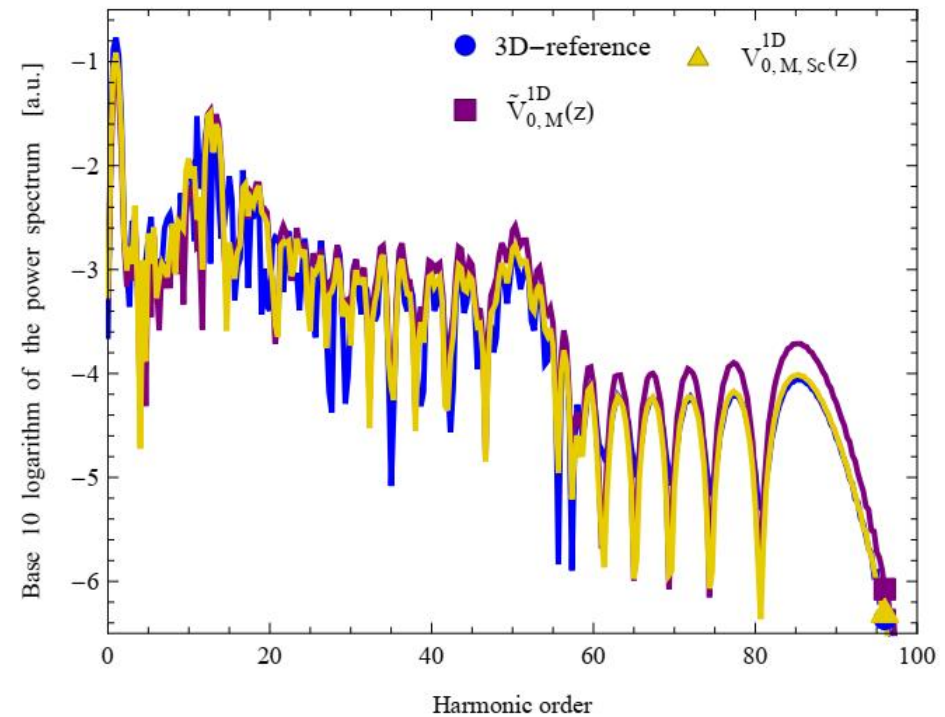
Figure 6. Panel (a): Logarithmic plot of the power spectra vs. the harmonic order, i.e.  $p(nf_1)$  (where  $f_1 = 1/T = 0.01$  a.u. is the fundamental frequency). Panel (b): Phase of the dipole acceleration spectra vs. the harmonic order (up shifted by  $2\pi$  for the 3D case). We plot the results for the density-based 1D model potential (purple) and for the improved soft-core Coulomb potential (gold) in comparison with the 3D reference (blue). The parameters  $F = 0.1$ ,  $N_{\text{Cycle}} = 3$ ,  $T = 100$  and  $Z = 1$  are the same as for Figs. 2 and 3.

HHG spectra:

H,  $3.51 \times 10^{14} \text{ W/cm}^2$

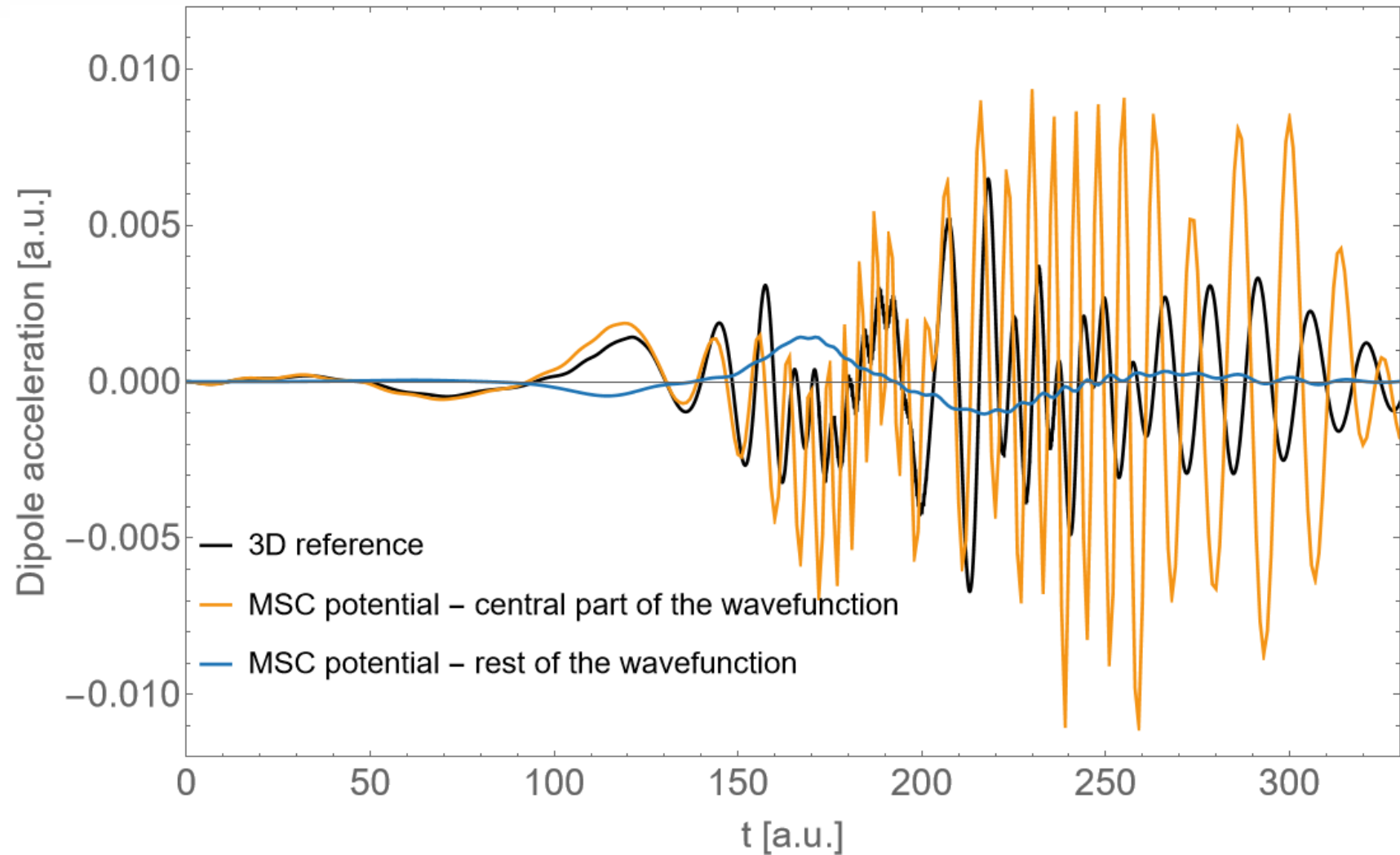
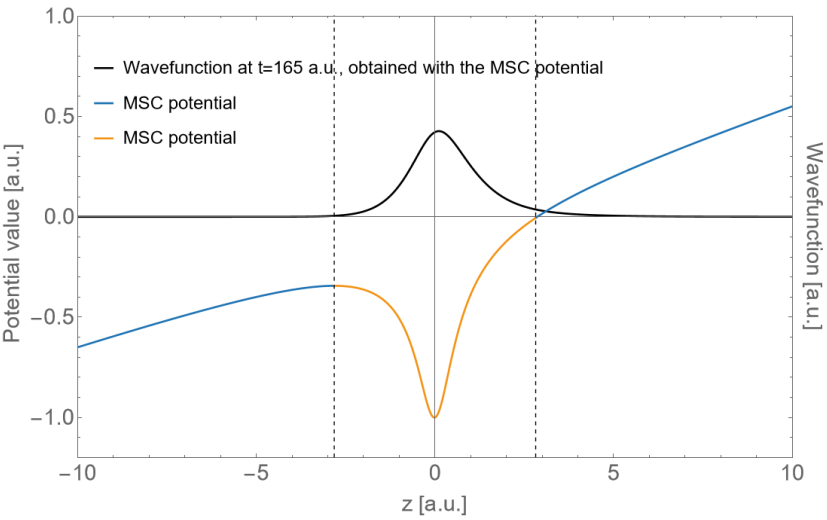


Ne (SAE),  $7.89 \times 10^{14} \text{ W/cm}^2$



Same simple scaling for power spectrum works for different SAE atoms and in a reasonable range of pulse intensities.

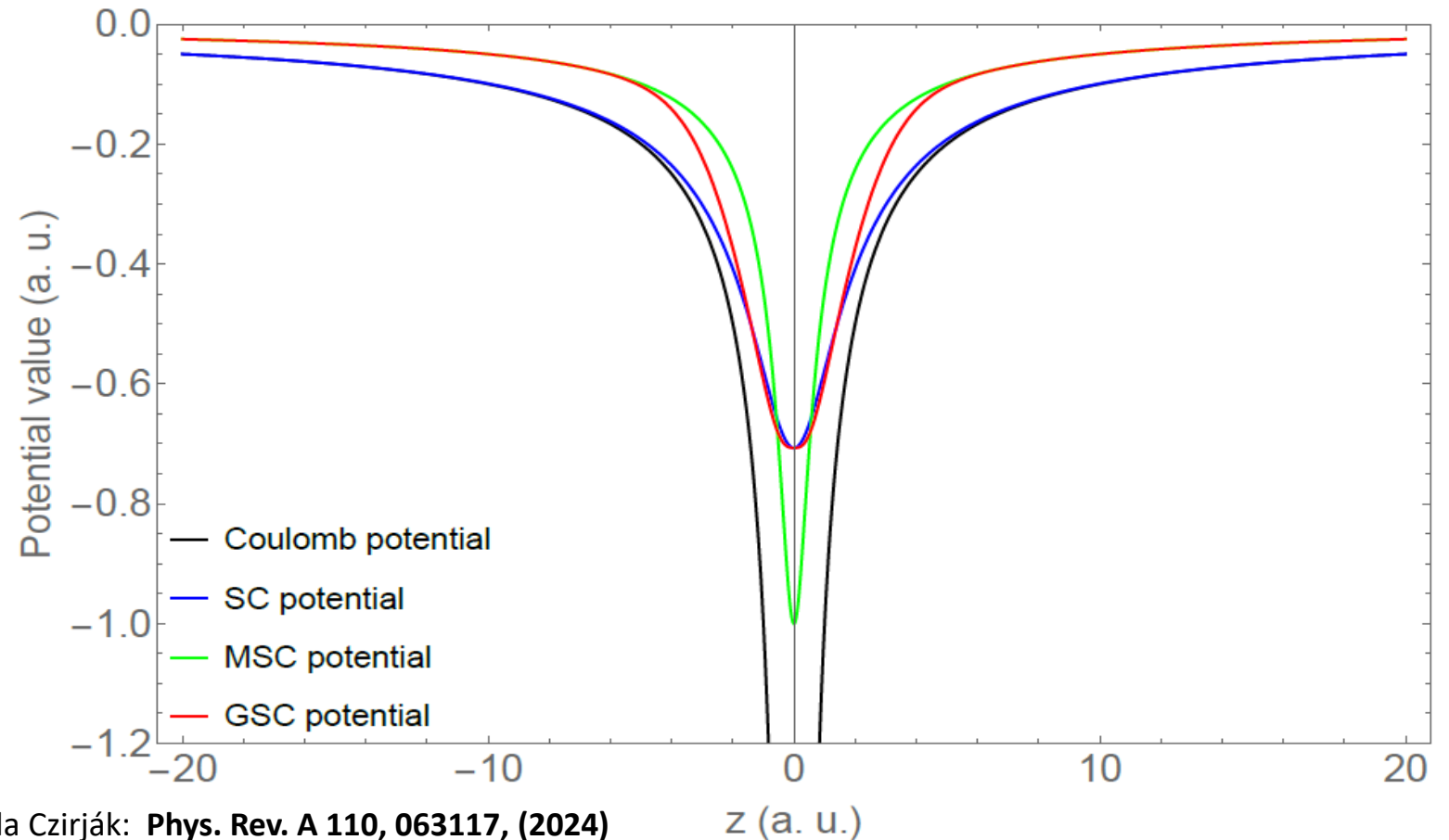
# Upgraded 1D atomic model potentials for HHG and simulation results



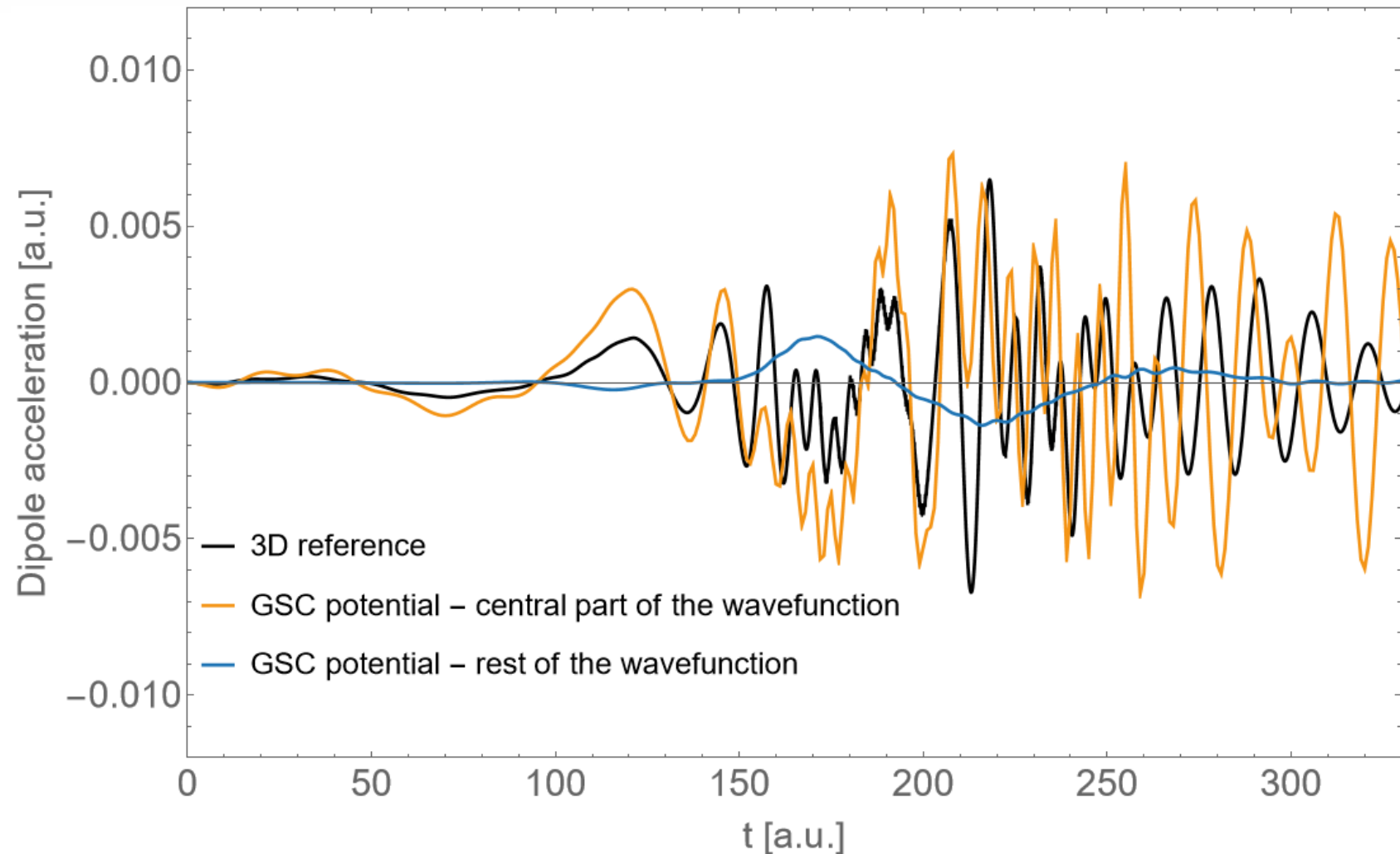
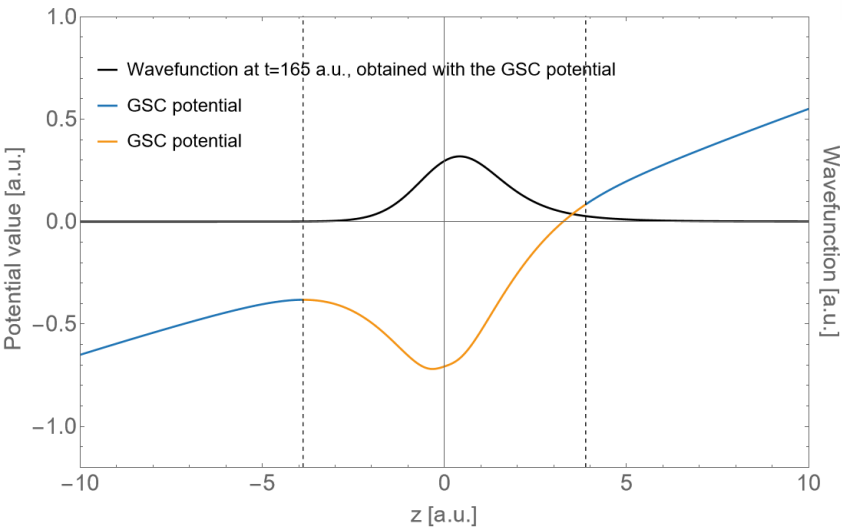
# The Gaussian windowed soft-core Coulomb (GSC) potential

$$V_{GSC}^{1D}(z) = V_{SC}^{1D}(z) \cdot e^{-(z/a)^2} + V_{MSC}^{1D}(z) \cdot \left(1 - e^{-(z/b)^2}\right)$$

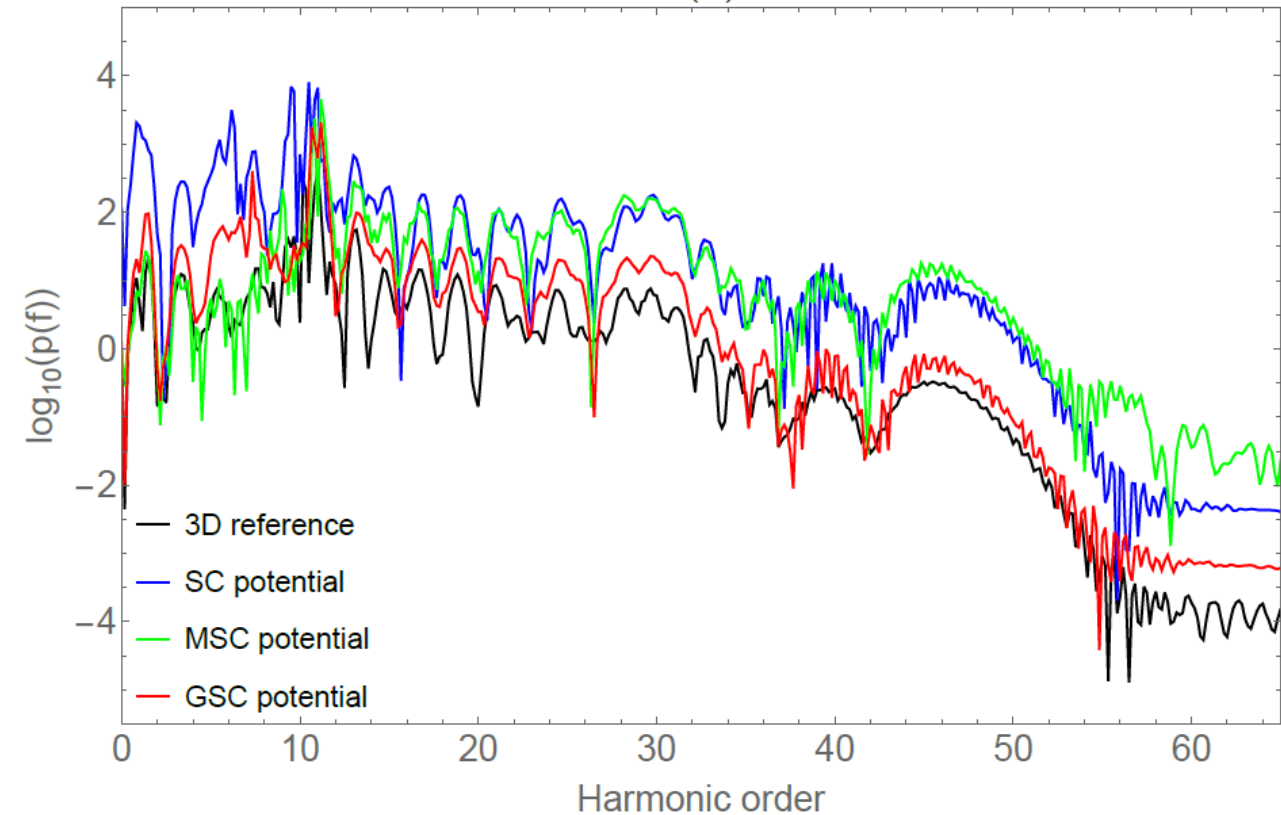
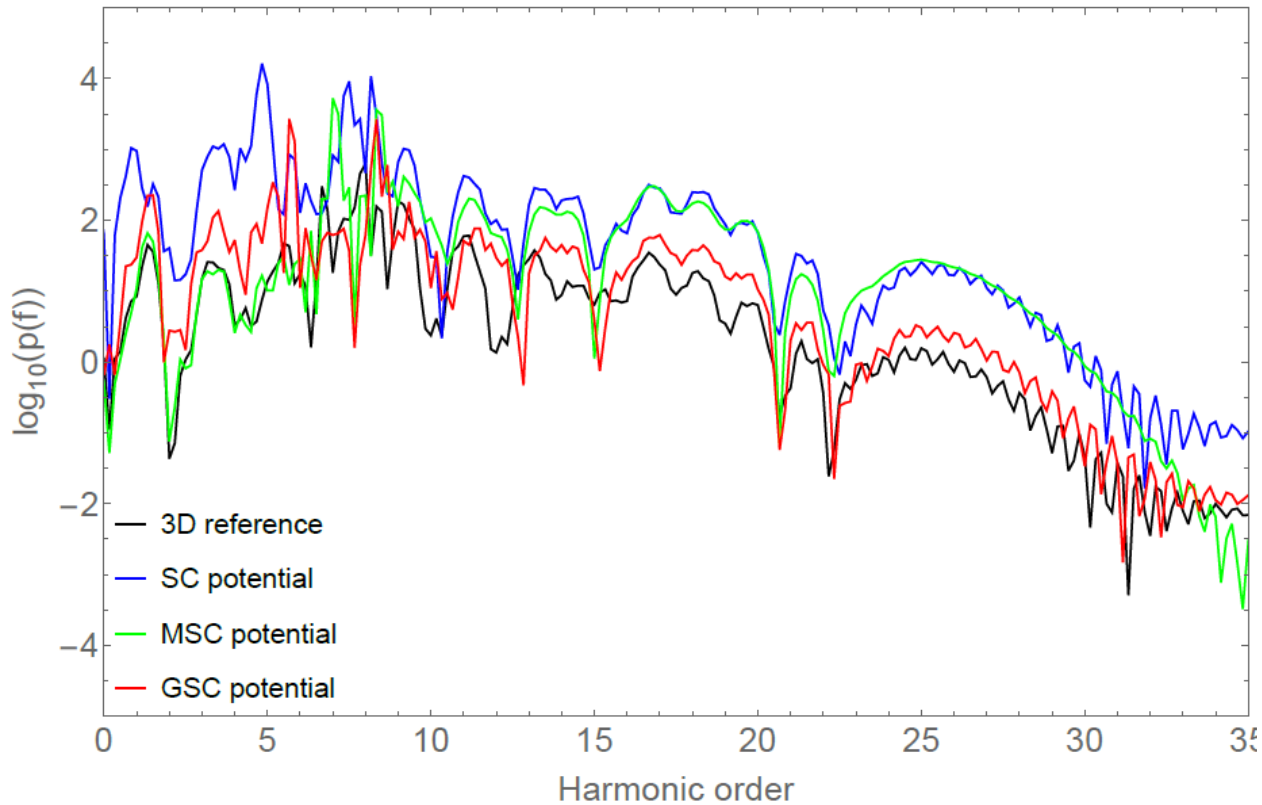
(with  $a = 2.551$  and  $b = 2$ .)



# The Gaussian windowed soft-core Coulomb (GSC) potential



# Hydrogen single atom HHG spectra simulated using GSC potential



The power spectrum of the dipole acceleration for hydrogen,  $N_C = 3$ ,  $F = 0.06$ ,

# Argon single atom HHG spectra simulated using GSC potential

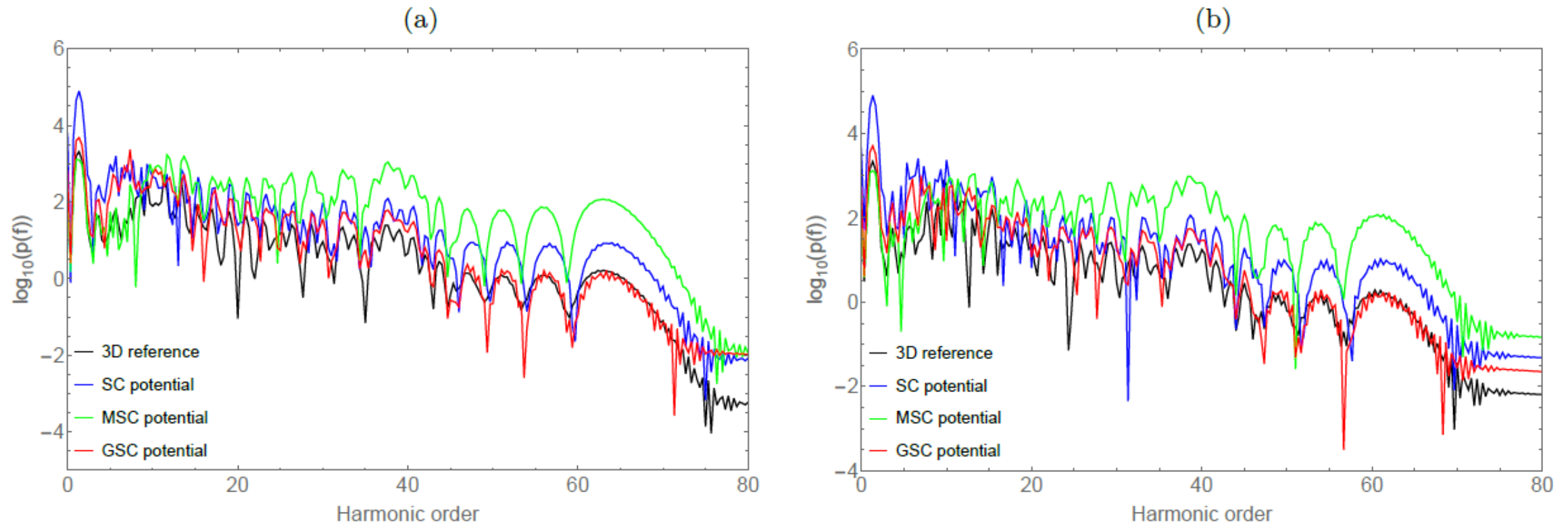


Figure 9. The power spectrum of the dipole acceleration for argon with  $T = 117$ ,  $N_C = 11$ ,  $F = 0.1$  with (a)  $k = 0$  and (b)  $k = 3.88 \cdot 10^{-6}$ .



# MMA-HHG code with GSC atomic model potential, running on Komondor

CUPRAD

- Parallel Radially Symmetric Unidirectional Solver
- Non-linear laser propagation

TDSE

- 1D-TSDE Implementation
- Microscopic response, **using GSC atomic model pot.**

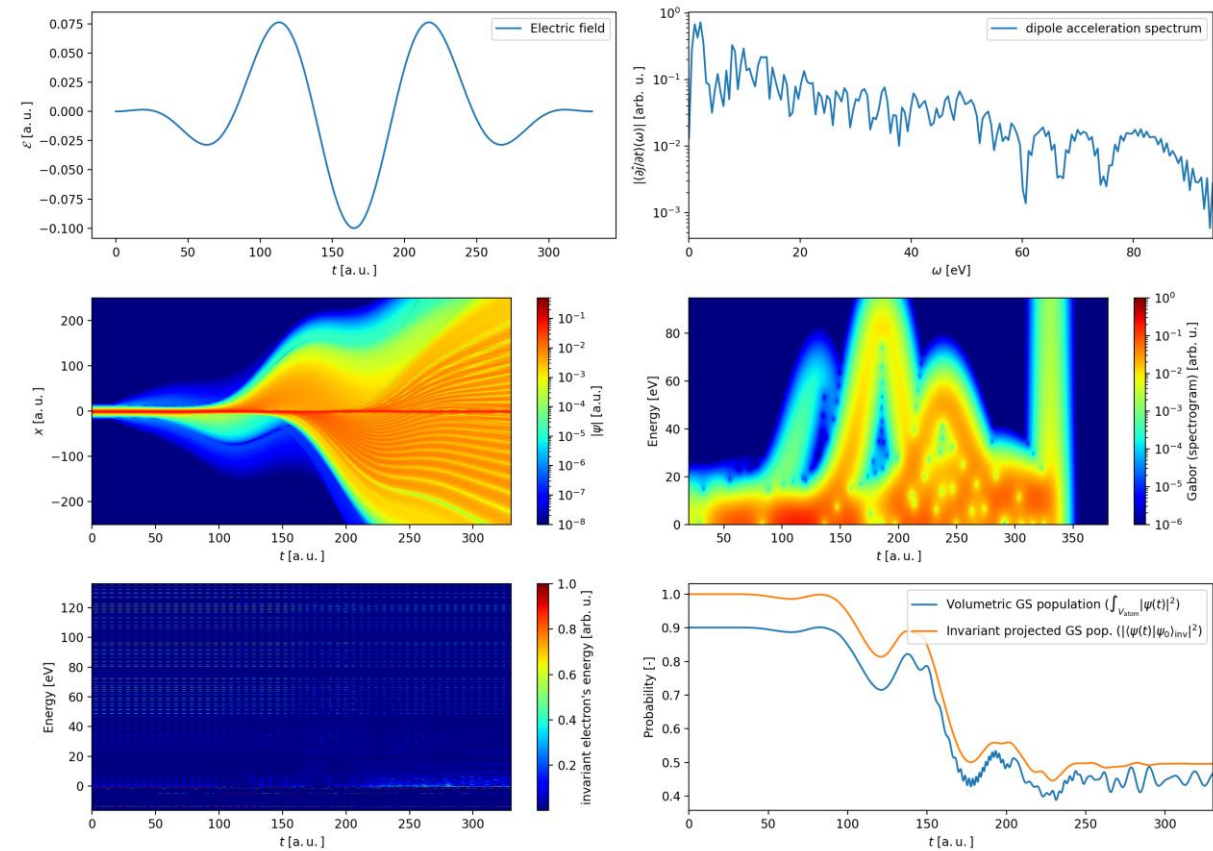
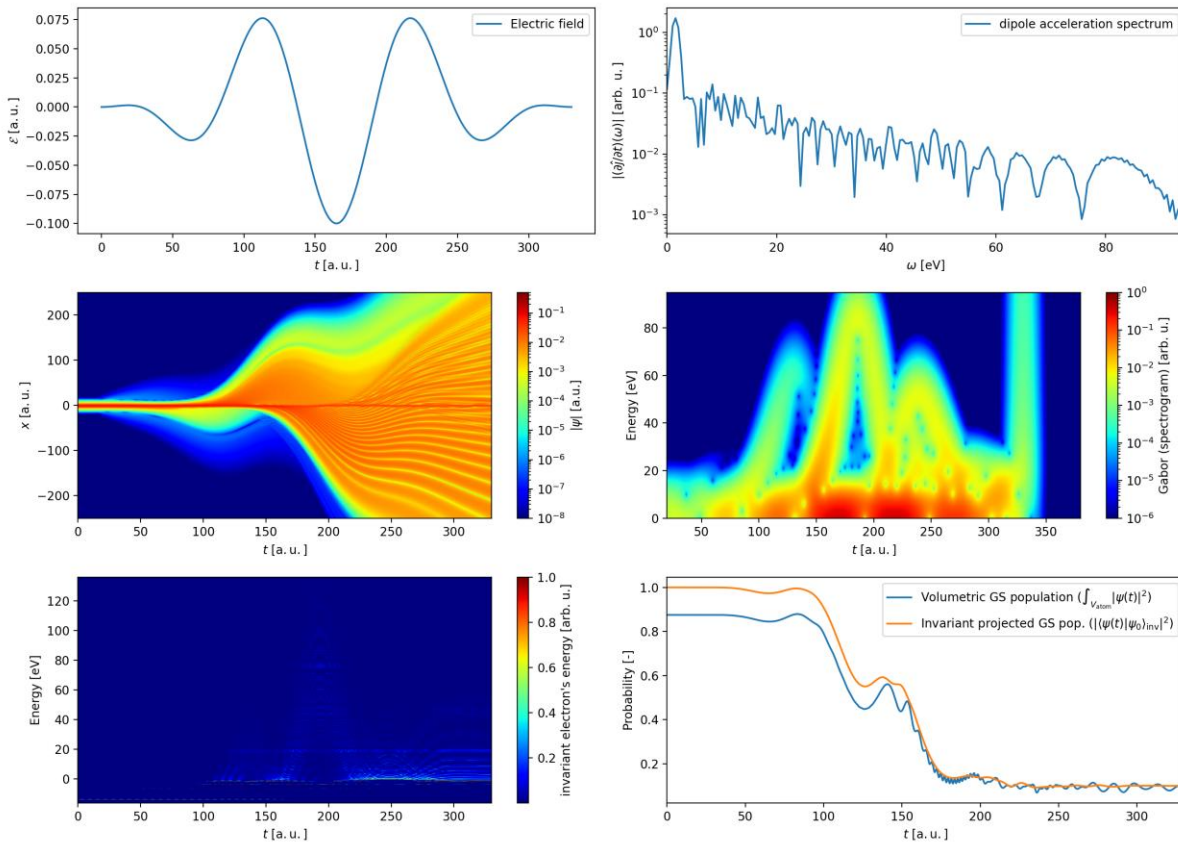
HANKEL

- Linear XUV Propagator
- XUV propagation

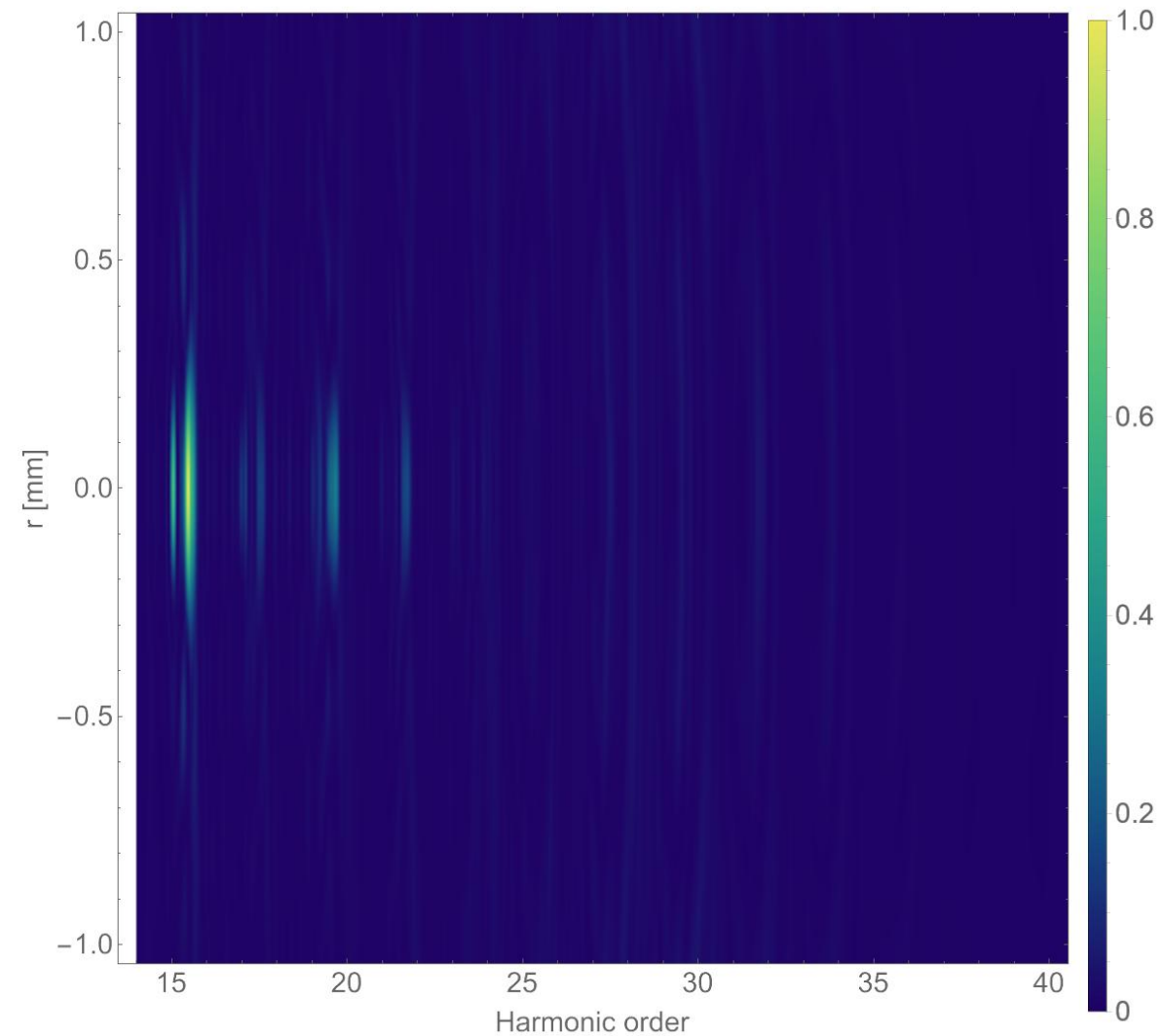
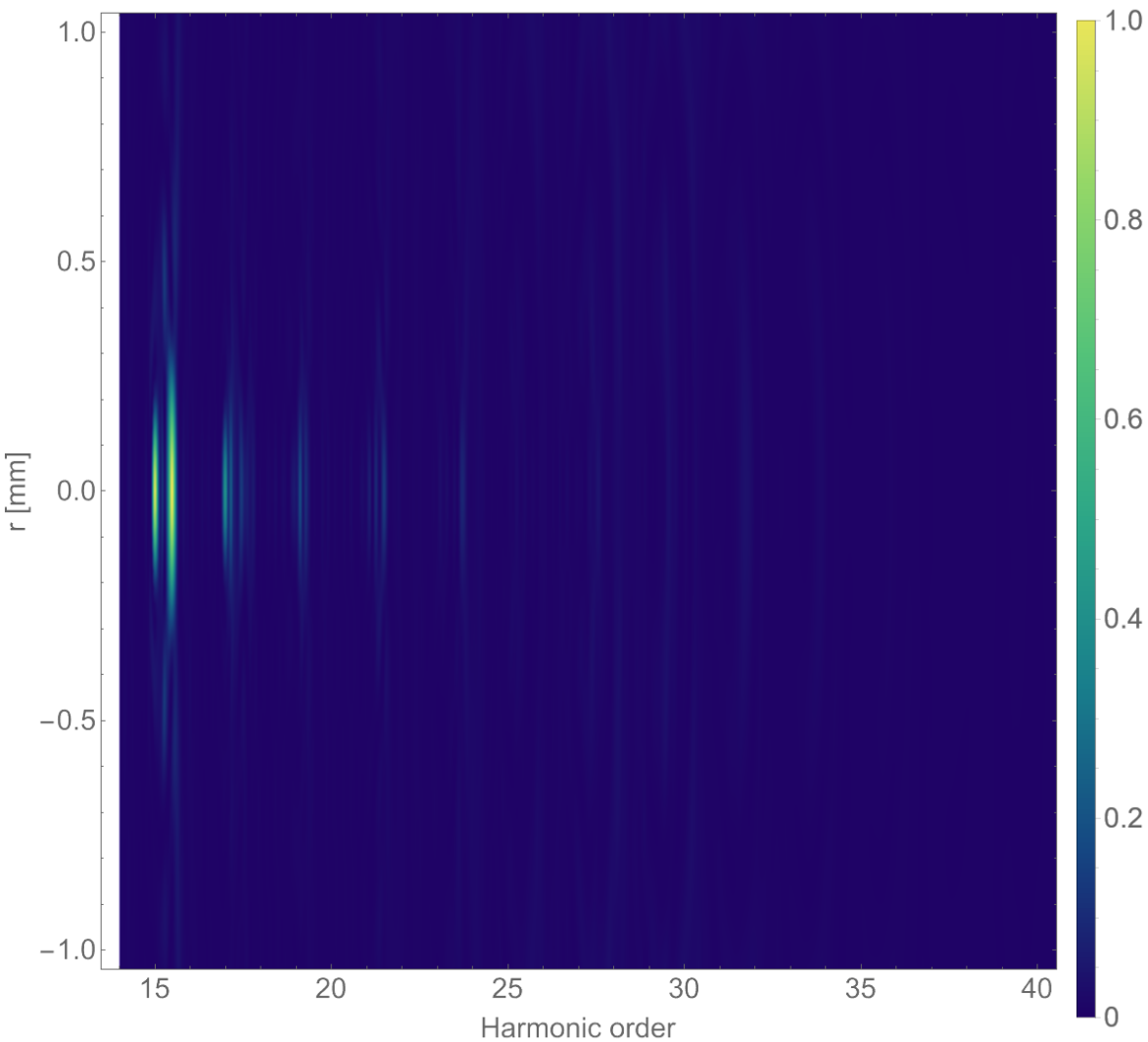
# Preliminary results by the MMA-HHG code using SC vs. GSC atomic potential

## SC

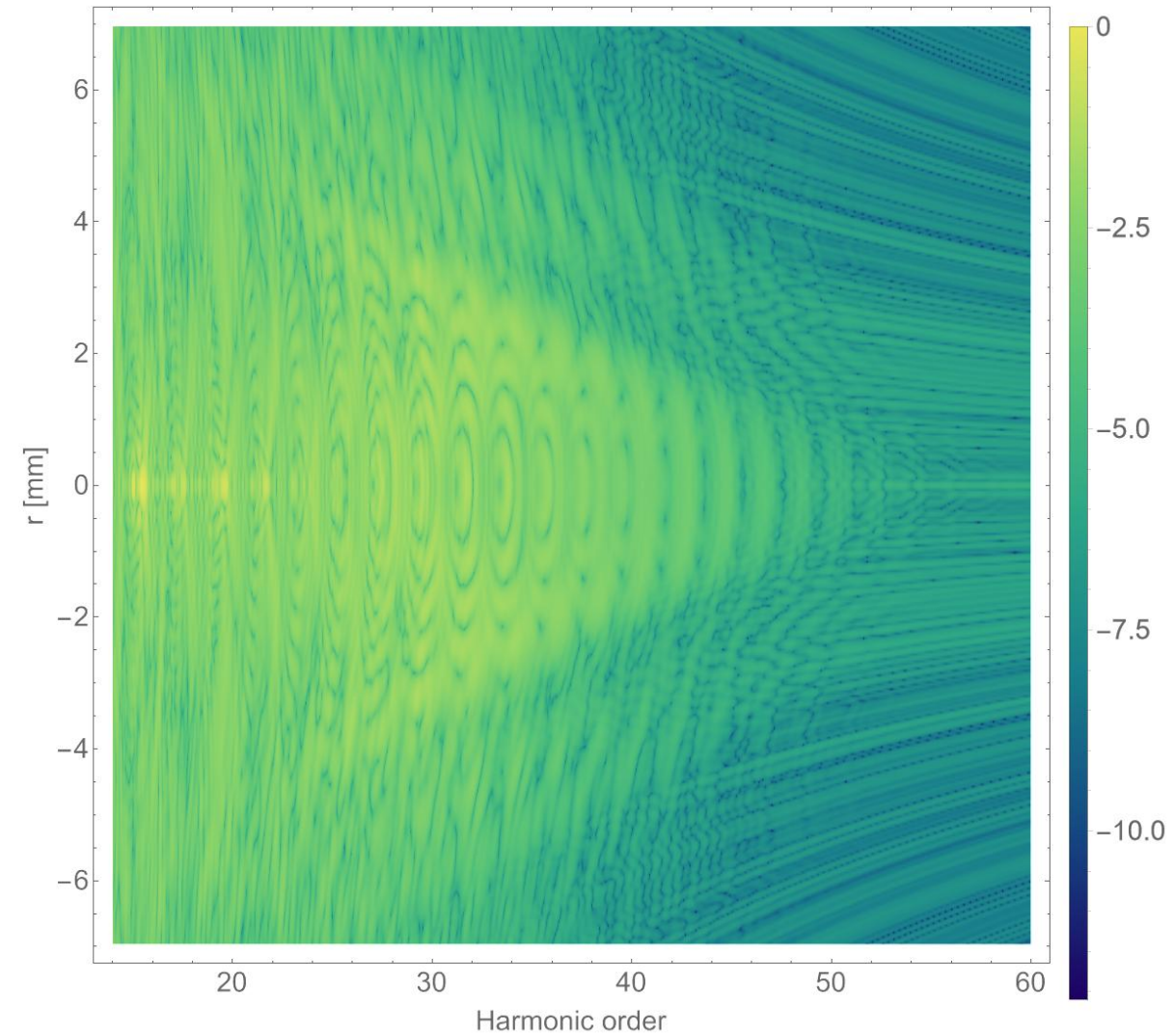
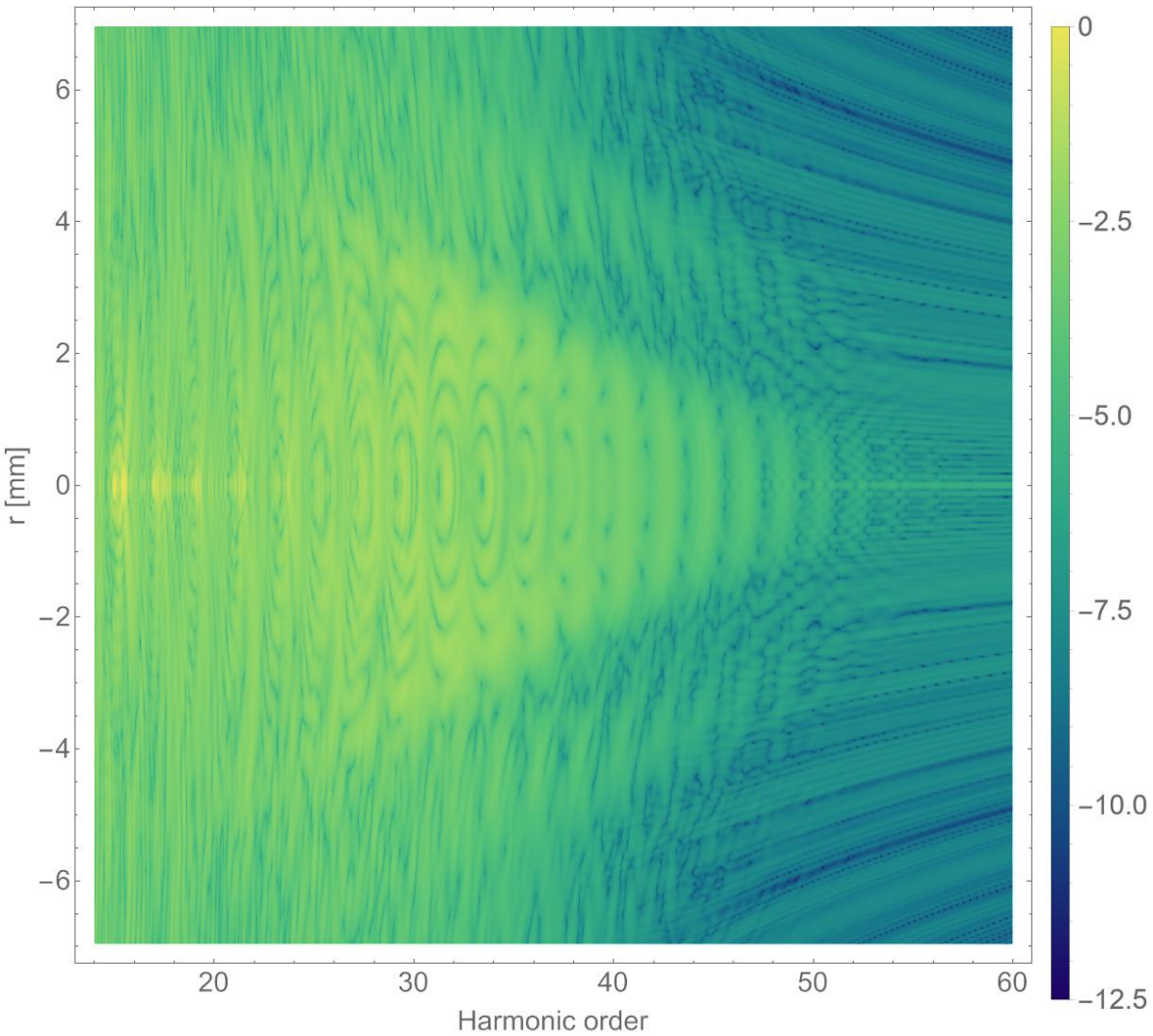
## GSC



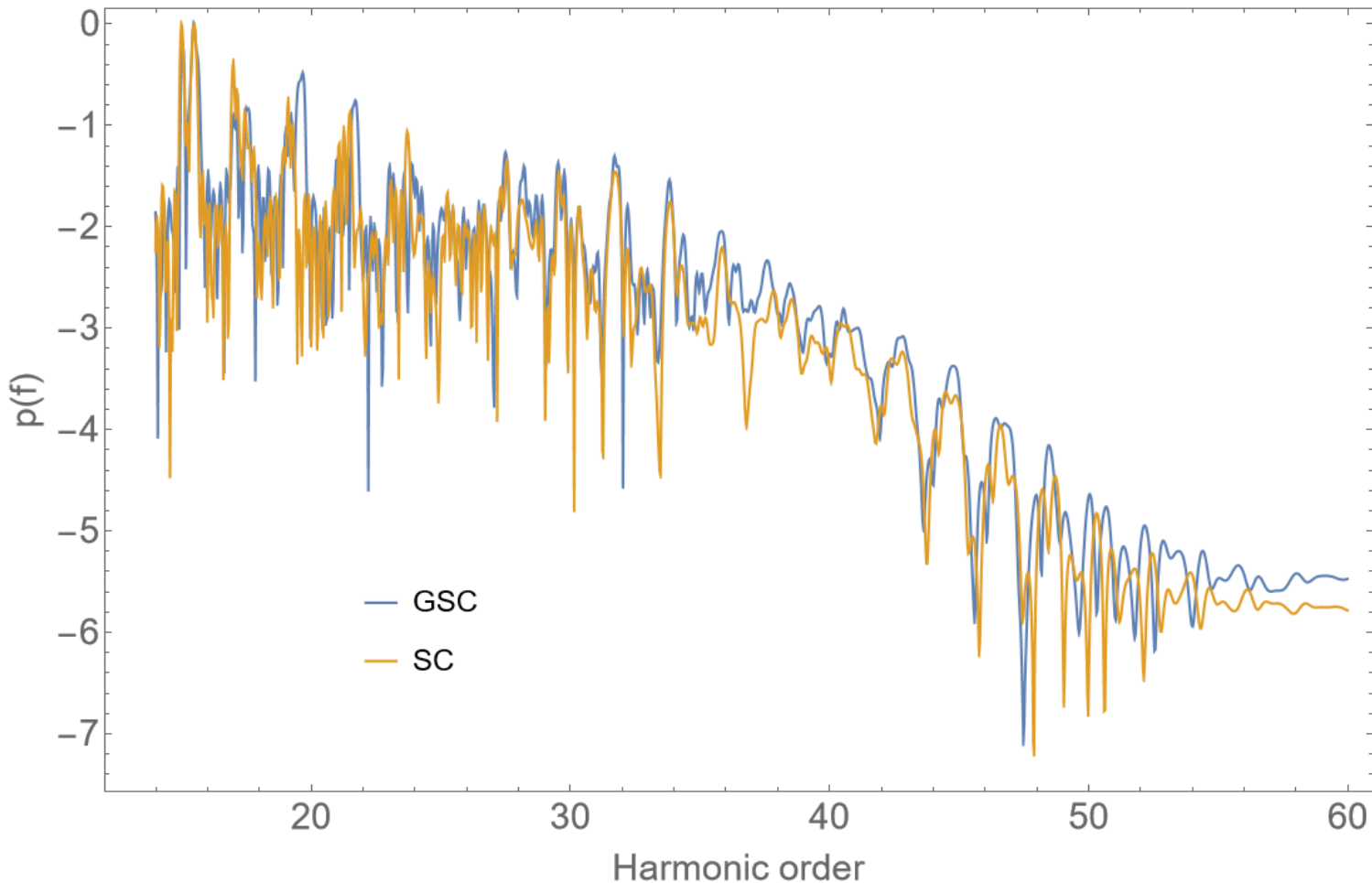
# Preliminary results by the MMA-HHG code using SC vs. GSC atomic potential



# Preliminary results by the MMA-HHG code using SC vs. GSC atomic potential



# Preliminary results by the MMA-HHG code using SC vs. GSC atomic potential



- Should enable direct comparison with experimental results
- Supercomputer load: TDSE solver parallel processing up to 1000s of CPU cores should be efficient
- Runtime for a medium with experimental relevance is close to upper limit at Komondor

# Summary and Acknowledgements



**Upgraded GSC 1D atomic model potentials enable efficient simulation of typical strong-field physics scenarios involving noble gas atoms driven by near- and mid-infrared laser pulses, with impressively increased accuracy compared to SC potentials.**

**The use of proper 1D atomic model potentials in the MMA-HHG code enables 1D TDSE-based numerical simulations of a macroscopic medium (low pressure gas jet or gas cell) and thus direct comparison of simulations and experiments.**

More details: Phys. Rev. A **98** (2018) 023401; Phys. Rev. A **101** (2020) 023405; Phys. Rev. A **110** (2024) 063117;

The ELI ALPS Project (GINOP-2.3.6-15-2015-00001) is supported by the European Union and co-financed by the European Regional Development Fund.

We acknowledge the Digital Government Development and Project Management Ltd. for awarding us access to the Komondor HPC facility based in Hungary.

**At last but not least,**



- PhD students, postdocs are welcome, both at ELI-ALPS and University of Szeged
- We are ready to help (also potential) users of ELI-ALPS with theory and simulation support
- Contact: [attila.czirjak@eli-alps.hu](mailto:attila.czirjak@eli-alps.hu)



THANK YOU  
FOR YOUR  
ATTENTION!

SZÉCHENYI 2020



HUNGARIAN  
GOVERNMENT

European Union  
European Regional  
Development Fund



INVESTING IN YOUR FUTURE